SIGNS OF UNPARTICLES AT COMPACT LINEAR COLLIDER

A THESIS SUBMITTED TO
THE GRADUATE SCHOOL OF NATURAL AND APPLIED SCIENCES
OF
MIDDLE EAST TECHNICAL UNIVERSITY

BY

CEMAL DİNÇ

IN PARTIAL FULFILLMENT OF THE REQUIREMENTS
FOR
THE DEGREE OF MASTER OF SCIENCE
IN
PHYSICS

SEPTEMBER 2019

Approval of the thesis:

SIGNS OF UNPARTICLES AT COMPACT LINEAR COLLIDER

submitted by **CEMAL DİNÇ** in partial fulfillment of the requirements for the degree of **Master of Science in Physics Department, Middle East Technical University** by,

Prof. Dr. Halil Kalıpçılar
Dean, Graduate School of **Natural and Applied Sciences** _____

Prof. Dr. Altuğ Özpineci
Head of Department, **Physics** _____

Prof. Dr. İsmail Turan
Supervisor, **Physics, METU** _____

Examining Committee Members:

Prof. Dr. Ali Ulvi Yılmazer
Physics Engineering, Ankara University _____

Prof. Dr. İsmail Turan
Physics, METU _____

Prof. Dr. Tahmasib M. Aliyev
Physics, METU _____

Prof. Dr. Altuğ Özpineci
Physics, METU _____

Assoc. Prof. Dr. Levent Selbuz
Physics Engineering, Ankara University _____

Date:

I hereby declare that all information in this document has been obtained and presented in accordance with academic rules and ethical conduct. I also declare that, as required by these rules and conduct, I have fully cited and referenced all material and results that are not original to this work.

Name, Surname: Cemal Dinç

Signature :

ABSTRACT

SIGNS OF UNPARTICLES AT COMPACT LINEAR COLLIDER

Dinç, Cemal
M.S., Department of Physics
Supervisor: Prof. Dr. İsmail Turan

September 2019, 67 pages

These are exciting times for particle physics since there has been tremendous advances recently. The most of all is the discovery of the long-sought Higgs boson at the Large Hadron Collider (LHC) in CERN. Even though this achievement completes the last missing piece of the Standard Model, the LHC would be far from to deliver its promises such as finding signs of physics beyond the Standard Model (also known as new physics) like low scale supersymmetry, extra dimensions etc. Unfortunately none of these hopes become a reality yet and expectations are not high. Therefore, studying other alternative new physics scenarios becomes important more than ever. One of such scenarios is known as unparticles. The idea is about a decade old and it is based on a scale invariant theory interacting with the Standard Model through effective field theory. The resulting theory reveal stuff that cannot be interpreted as particles which is why the notion of unparticle has been introduced. First the idea of conformal symmetry will be discussed in some detail. Then after a brief description of the effective field theory in general, the idea of unparticles will be presented with more emphasis on the scalar version of unparticles. It will be assumed that unparticles decay within the detector so that only their virtual effects to various signals at

the Compact Linear Collider. For that purpose, the model is implemented in computational software `Madgraph` so that a signal analysis is carried out with the help of the software `MadAnalysis`. A comparison with the Standard Model is done.

Keywords: effective field theory, conformal invariance, unparticles, multiphoton signals, Compact Linear Collider (CLIC)

ÖZ

KOMPAKT LİNEER ÇARPIŞTIRICIDA APARÇACIK İZLERİ

Dinç, Cemal
Yüksek Lisans, Fizik Bölümü
Tez Yöneticisi: Prof. Dr. İsmail Turan

Eylül 2019 , 67 sayfa

Yakın zamandaki muazzam gelişmelerle beraber, parçacık fiziği heyecan verici bir dönem yaşıyor. Bu gelişmelerin en önemlisi uzun süreden beridir aranan Higgs bozonunun LHC'deki keşfi oldu. Her ne kadar bu başarı Standart Model'in son kayıp halkasını tamamlasa da, Büyük Hadron Çarpıştırıcısı (BHÇ) süpersimetri, ekstra boyutlar gibi Standart Model ötesi teorilerin izlerini bulma amacını yerine getirmekten uzakta görünüyor. Maalesef umut edilenlerin hiçbiri henüz gerçek olamadı ve bu konuda beklentiler hiç yüksek görünmüyor. Bundan dolayı, farklı alternatif yeni fizik senaryoları her zamankinden daha önemli bir hale geldi. Bu gibi senaryolardan birisi Aparçacıklardır. Bu fikir yaklaşık olarak on yıl önce öne sürüldü ve etkin alan teorisi yoluyla Standart Model ile etkileşen ölçekleme değişmezliği teorisine dayanıyor. Ortaya çıkan teori parçacık olarak yorumlanmayacak şeyleri öne sürmesinden dolayı Aparçacık kavramı tanımlandı. Bu tezde, ilk olarak konform (açı-korur) simetri detaylıca tartışıldı. İkinci olarak, kısa bir etkin alan teorisi tanımından sonra aparçacık fikri özellikle skaler aparçacıklar üzerinde durularak sunuldu. Aparçacıkların dedektörün içinde bozulduğu varsayıldı ve Kompakt Lineer Çarpıştırıcında bulunması olası sinyallerdeki sanal etkilerine bakıldı. Bu amaç için model hesaba dayalı

yazılım programı `Madgraph`'a yerleştirildi. Böylece sinyal analizi, yazılım programı `MadAnalysis` aracılığı ile yerine getirildi. Standart Model ile karşılaştırılması yapıldı.

Anahtar Kelimeler: etkin alan teorisi, konformal değişmezlik, aparçacıklar, çoklu foton sinyalleri, Kompakt Lineer Çarpıştırıcısı

To my family

ACKNOWLEDGMENTS

I would like to thank my supervisor, Prof. Dr. İsmail Turan for his insight, patience, motivation and immense knowledge. His guidance helped me in all time of research and writng of this thesis.

I must express my very profound gratitude to my family for their unconditional support and continuous encouragement throughout writing this thesis and my life in general. This accomplishment would not be possible without them. I would also like to thank my friends for their encouragement and friendship.

TABLE OF CONTENTS

LIST OF TABLES

TABLES

LIST OF FIGURES

FIGURES

LIST OF ABBREVIATIONS

BSM	Beyond Standard Model
BZ	Banks-Zaks
CFT	Conformal Field Theory
CLIC	Compact Linear Collider
EFT	Effective Field Theory
ILC	International Linear Collider
LHC	Large Hadron Collider
SM	Standard Model

CHAPTER 1

INTRODUCTION

The Standard Model (SM) of particle physics is a monumentally successful theory to describe three of the four fundamental forces, namely the electromagnetic, weak and strong forces. The SM very accurately describes all existing data and predicts properties of particles and their interactions. In 2012, Higgs particle, which had been searched for decades, has been discovered independently by two experimental collaborations at Large Hadron Collider (LHC) at CERN [1, 2] that has been searched for many years. Even though its great achievements, the SM is not believed to be a complete theory of particle physics, since there are still many unresolved issues. For instance, the SM is not able to provide a mechanism for neutrino mass. The cosmological observations indicate that the SM can only determine 4% of all matter in the universe and yet there is not any dark matter candidate within the SM. Also, the SM does not contain gravitation interactions which is the most notable force in our daily life.

There are several valid candidates for the physics beyond the SM, known as "new physics". The new physics may be weakly coupled like super-symmetric theories or may be strongly coupled like technicolor. There could be a third option that the new physics can be conformal invariant.

About a decade ago, Georgi introduced the notion of unparticle physics [3,4]. "Unparticle physics describes a situation in which standard model physics is weakly coupled, at high energies, to a sector that flows to a scale-invariant theory in the infrared" [5]. Unparticles are mostly studied either through their direct production or through the unparticle propagator. In this thesis, we solely focus on virtual effects of unparticles.

Unparticle theory is phenomenologically rich and because of the conformal symmetry, the theory foresee the possibility of unparticle self interactions [6–11]. Unparticle self interactions lead to signals with various four particle final states such as 4γ, $2\gamma 2g$, $2\gamma 2l$, $4l$. Additionally, single or double unparticle exchange diagrams can make important contributions to these signals. Therefore we consider complete evaluation of such signals including all contributions.

Theoretical and phenomenological studies have been done on unparticle stuff in many different areas such as atomic physics [12,13], dark matter [14,15], AdS/CFT [16,17], cosmology [18–20] and condensed matter physics [21–23] . A search for unparticle effects is studied through their real emissions at LHC [24, 25]. The analysis is performed using events containing two leptons. The signal is associated production of unparticle and Z-boson.

The thesis is organized as follows. In chapter 2, we review much of the theoretical background required for understanding unparticle theory. In the first part of this chapter Conformal Field Theory (CFT) is studied in general. The conformal group, its generators and both classical and quantum mechanical interpretation of CFT are discussed in detail. The essentials for Effective Field Theory (EFT) are introduced. We finalize this chapter with a brief explanation of Banks-Zaks (BZ) fixed point.

In chapter 3, we describe the unparticle model. The interaction of unparticles with Standard Model fields and related Feynman rules are given. The elements required for a reasonable unparticle theory; phase space of unparticles and unparticle propagator are introduced.

In chapter 4, the numerical analysis of processes with four-particle compositions in final states is performed and the results are presented. In chapter 5, the summary of the thesis is given.

CHAPTER 2

THEORETICAL OVERVIEW

2.1 Conformal Field Theory

In this section, we describe the conformal field theory and conformal symmetry with some details. We closely follow the book by Francesco, Mathieu and Sénéchal [26].

2.1.1 Conformal transformations in d dimensions

Conformal transformations, in general, are coordinate transformations that preserve the angle between two vector fields u and v, but not necessarily preserve their lengths;

$$cos(\theta_{\angle(u,v)}) = \frac{u.v}{\|u\| \, \|v\|} \tag{2.1}$$

where $u.v = g_{\mu\nu}u^{\mu}v^{\nu}$ and $\|u\| = \sqrt{g_{\mu\nu}u^{\mu}u^{\nu}}$.

Let us consider a manifold M, $M = \mathbb{R}^d$ where $d = p + q$ and the flat metric which is defined as $\eta_{\mu\nu} = g_{\mu\nu} = diag(\underbrace{+1, +1, +1, ..}_{\text{p}}, \underbrace{-1, -1, -1, ..}_{\text{q}}), \quad p, q \in Z^+$.

A conformal transformation can be considered as a smooth change of coordinates that leaves the metric invariant up to an overall scale factor $\omega(x)$. In other words;

$$x \to x' \equiv x'(x) \quad \text{where} \quad x = (x^1, x^2, ..., x^p, x^{p+1}, ..., x^{p+q})$$

such that

$$g_{\mu\nu} \to g'_{\mu\nu}(x') = \frac{\partial x^{\rho}}{\partial x'^{\mu}} . \frac{\partial x^{\delta}}{\partial x'^{\nu}} \; g_{\delta\rho} \tag{2.2}$$

where

$$g'_{\mu\nu} = \omega(x) g_{\mu\nu} \ , \ \omega(x) > 0. \tag{2.3}$$

2.1.2 The Conformal Group in d Dimensions

A set of conformal transformations construct the so-called conformal group, denoted as $conf(M)$, which is the connected component containing the identity in the group of all conformal transformations of M.

Let us now classify group $G = conf(\mathbb{R}^{p+q})$ by using only the infinitesimal form of the transformation. Consider an infinitesimal coordinate transformation,

$$x^\mu \to x^\mu + \epsilon^\mu.$$

Under the circumstances, metric changes as

$$g'_{\mu\nu}(x') = \frac{\partial x^\alpha}{\partial x'^\mu} . \frac{\partial x^\beta}{\partial x'^\nu} \ g_{\beta\alpha} \ . \tag{2.4}$$

The first partial derivative can be written as,

$$\frac{\partial x^\alpha}{\partial x'^\mu} = \frac{\partial (x'^\alpha - \epsilon^\alpha)}{\partial x'^\mu} = \delta^\alpha_\mu - \partial_\mu \epsilon^\alpha. \tag{2.5}$$

Similarly we have

$$\frac{\partial x^\beta}{\partial x'^\nu} = \delta^\beta_\nu - \partial_\nu \epsilon^\beta \ . \tag{2.6}$$

Hence the metric becomes

$$g'_{\mu\nu} = [\delta^\alpha_\mu - \partial_\mu \epsilon^\alpha][\delta^\beta_\nu - \partial_\nu \epsilon^\beta] \ \ g_{\alpha\beta}. \tag{2.7}$$

The transformed metric up to order $O(\epsilon)$ is

$$g'_{\mu\nu} = g_{\mu\nu} - \partial_\mu \epsilon_\nu - \partial_\nu \epsilon_\mu \ . \tag{2.8}$$

This equation manifestly implies that if the transformation is conformally invariant $\partial_\mu \epsilon_\nu + \partial_\nu \epsilon_\mu$ should be proportional to $g_{\mu\nu}$. So, we have the following relation

$$\partial_\mu \epsilon_\nu + \partial_\nu \epsilon_\mu = f(x) . g_{\mu\nu} \ . \tag{2.9}$$

In order to find f(x), we multiply both sides by $g^{\mu\nu}$;

$$2(\partial . \epsilon) = f(x) g^{\mu\nu} g_{\mu\nu} = f(x) d$$

Then,

$$f(x) = \frac{2}{d}(\partial.\epsilon). \tag{2.10}$$

Finally we obtain,

$$\partial_\mu \epsilon_\nu + \partial_\nu \epsilon_\mu = \frac{2}{d}(\partial.\epsilon) g_{\mu\nu} \ . \tag{2.11}$$

Hence the overall scale factor $\omega(x)$ is

$$\omega(x) = 1 - \frac{2}{d}(\partial.\epsilon) \ . \tag{2.12}$$

It is not hard to see that if we check (2.11) for $d = 1$, the equation will provide trivial solutions. Next step is to multiply (2.11) with $\partial^\mu \partial^\nu$. We will get

$$\partial^\mu \partial^2 \epsilon_\mu + \partial^\nu \partial^2 \epsilon_\nu = \partial^2 \frac{2}{d} \ (\partial.\epsilon) \tag{2.13}$$

which leads to

$$\partial^2(\partial.\epsilon) = \frac{1}{d}\partial^2(\partial.\epsilon) \ . \tag{2.14}$$

Therefore, for $d > 1$ we obtain

$$\partial^2(\partial.\epsilon) = 0 \tag{2.15}$$

This time let us contract (2.11) with $\partial_\lambda \partial^\nu$. We have

$$\partial^2 \partial_\lambda \epsilon_\mu + \big(1 - \frac{2}{d}\big)\partial_\lambda \partial_\mu (\partial.\epsilon) = 0 \tag{2.16}$$

Now if we interchange the indices λ, μ in eq (2.16) and add this new equation to (2.16), we get

$$\partial^2.(\partial_\lambda \partial_\mu + \partial_\mu \partial_\lambda) + 2\big(1 - \frac{2}{d}\big)\partial_\lambda \partial_\mu (\partial.\epsilon) = 0 \ . \tag{2.17}$$

Furthermore, by using (2.11), we can see that

$$\frac{1}{d}\partial^2 \ g_{\mu\lambda} \ (\partial.\epsilon) + \big(1 - \frac{2}{d}\big)\partial_\lambda \partial_\mu (\partial.\epsilon) = 0 \ . \tag{2.18}$$

The first term will cancel due to (2.15). Therefore the equation turns into

$$\big(1 - \frac{2}{d}\big)\partial_\lambda \partial_\mu (\partial \cdot \epsilon) = 0 \ . \tag{2.19}$$

For $d > 2$ we have

$$\partial_\lambda \partial_\mu (\partial.\epsilon) = 0 \tag{2.20}$$

Even from this equation we can deduce that $d = 2$ needs a special treatment. The following step is to multiply (2.11) this time by $\partial_\lambda \partial_\rho$. This yields

$$\partial_\lambda \partial_\rho \partial_\mu \epsilon_\nu + \partial_\lambda \partial_\rho \partial_\nu \epsilon_\mu = \frac{2}{d}\, g_{\mu\nu}\, \partial_\lambda \partial_\rho . (\partial . \epsilon) \ . \tag{2.21}$$

The right hand side is zero because of (2.20). If we define $\partial_\lambda \partial_\rho \partial_\mu \epsilon_\nu \equiv \Delta_{\lambda\rho\mu\nu}$, (2.21) can be rewritten as

$$\Delta_{\lambda\rho\mu\nu} = -\Delta_{\lambda\rho\nu\mu} \ . \tag{2.22}$$

So, we can conclude that $\Delta_{\lambda\rho\mu\nu}$ is symmetric in the first three indices and anti-symmetric in last two indices.

However with these symmetries, it can be indicated that Δ have to be zero;

$$\Delta_{\lambda\rho\mu\nu} = \Delta_{\lambda\mu\rho\nu} = -\Delta_{\lambda\mu\nu\rho} = -\Delta_{\lambda\nu\mu\rho} = \Delta_{\lambda\nu\rho\mu} = \Delta_{\lambda\rho\nu\mu} \ . \tag{2.23}$$

As a result,

$$\boxed{\Delta_{\lambda\rho\mu\nu} = 0}$$

That is why, $\partial_\lambda \partial_\rho \partial_\mu \epsilon_\mu = 0$. So, almost instantly it can be seen that as the third derivative of ϵ vanishes, it should be at most quadratic in x. Hence, ϵ^μ, in general, can be written as follows,

$$\epsilon^\mu = a^\mu + b^\mu_\nu \, x^\nu + c^\mu_{\nu\lambda} \, x^\nu x^\lambda \ . \tag{2.24}$$

Now let us insert ϵ^μ to (2.11). Each order of x can be treated separately, since they are linearly independent. At first order we obtain

$$\mathcal{O}(x) : b_{\mu\nu} + b_{\nu\mu} = \frac{2}{d} b^\lambda_\lambda \, g_{\mu\nu}. \tag{2.25}$$

$b_{\mu\nu}$ may be separated into a symmetric and an anti-symmetric part;

$$b_{\mu\nu} = \xi_{\mu\nu} + \Lambda_{\mu\nu} \ . \tag{2.26}$$

So, at first order in x, we have

$$\xi_{\mu\nu} = \frac{1}{d} \xi^\lambda_\lambda g_{\mu\nu} \ . \tag{2.27}$$

The symmetric part $\xi_{\mu\nu}$ is proportional to metric $g_{\mu\nu}$ and there is no restriction in anti-symmetric part. At second order in x,

$$\mathcal{O}(x^2) : c_{\mu\nu\rho} + c_{\nu\mu\rho} = \frac{2}{d} \, c^\lambda_{\lambda\rho} \ g_{\mu\nu} \ . \tag{2.28}$$

It can also be written as

$$c_{\mu\nu\rho} = -c_{\nu\mu\rho} - 2h_\rho\, g_{\mu\nu} \quad \text{where} \quad h_\rho = -\frac{1}{d} c^{\lambda}_{\lambda\mu} \tag{2.29}$$

$$c_{\mu\nu\rho} = -c_{\mu\nu\rho} - 2h_\rho\, g_{\mu\nu} + 2h_\mu\, g_{\nu\rho} - 2h_\nu\, g_{\mu\rho} \tag{2.30}$$

Therefore,

$$c_{\mu\nu\rho} = h_\rho\, g_{\mu\nu} + h_\mu\, g_{\nu\rho} + h_\nu\, g_{\mu\rho}\,. \tag{2.31}$$

To sum up, what we have learned here is

at	$\mathcal{O}(x^0):$	$\epsilon^\mu = a^\mu:$ constant $\Rightarrow$	Space - time translations
at	$\mathcal{O}(x^1):$	$(i)\ \epsilon^\mu = \omega^\mu_\nu x^\mu:$ anti-symm. tensor $\Rightarrow$	Rotations
at	$\mathcal{O}(x^1):$	$(ii)\ \epsilon^\mu = \lambda x^\mu:\ (\lambda > 0) \Rightarrow$	Scale Transformations
at	$\mathcal{O}(x^2):$	$\epsilon^\mu = h^\mu x^2 - 2x^\mu\,(h.x) \Rightarrow$	(SCTs)

The special conformal transformation (SCT) is a sequence of inversion, translation and inversion again. Under inversion transformation coordinates change as $x \to x/x^2$. We can observe that the Poincare group is just a subgroup of conformal group. It may also be said that every conformal invariant theory is simultaneously scale invariant, but the converse does not have to be true.

To obtain the global conformal transformations, we need to exponentiate the infinitesimal transformations. They can be described as follows,

i. Translation: $x^\mu \to x^\mu + c^\mu \quad c \in \mathbb{R}^d$

ii. Lorentz transformation: $x^\mu \to \Lambda^\mu_\nu x^\nu \quad \Lambda \in O(p,q)$

iii. Dilation: $x^\mu \to \lambda x^\mu \quad \lambda \in \mathbb{R}^+$

iv. SCT: $x^\mu \to \dfrac{x^\mu - h^\mu x^2}{1 - 2hx + h^2x^2}$

For each case the scale factor can be determined. For the first two, the scale factor is equal to the identity. The scale factor of dilations and SCTs is $\omega(x) = \lambda^{-2}$ and $(1 - 2hx + h^2x^2)^2$, respectively.

2.1.3 Conformal Transformations in $d = 2$

In an Euclidean space, i.e., $g_{\mu\nu} = \delta_{\mu\nu}$, (2.11) turns into Cauchy-Riemann equations,

$$\partial_1\varepsilon_1 = \partial_2\varepsilon_2 \quad and \quad \partial_1\varepsilon_2 = -\partial_2\varepsilon_1 \ . \tag{2.32}$$

By using this transformations, we can introduce complex coordinates

$$\sigma = x_1 + ix_2 \quad \bar{\sigma} = x_1 - ix_2 \tag{2.33}$$

and

$$\varepsilon(\sigma) = \varepsilon_1 + i\varepsilon_2 \quad and \quad \bar{\varepsilon}(\sigma) = \varepsilon_1 - i\varepsilon_2 \quad \text{can be written.} \tag{2.34}$$

$d = 2$ global conformal transformations correspond to holomorphic functions,

$$\sigma \to f(\sigma) \quad \text{where} \quad f(\sigma) = \alpha\sigma + \beta \qquad \bar{\sigma} \to \bar{f}(\bar{\sigma}) \ .$$

Therefore, in $2d$

$$ds^2 = d\sigma d\bar{\sigma} \to \left|\frac{\partial f}{\partial \sigma}\right|^2 d\sigma d\bar{\sigma} \quad \text{where} \quad \omega(x) = \left|\frac{\partial f}{\partial \sigma}\right|^2$$

2.1.4 Classical Conformal Field Theory

In this section we study the local conformal transformations. In order to do that we need to have a collection of observable $\phi_a(x)$ which is labeled by space time point $x \in \mathbb{R}$ and $a \in I$ where I is the index set.

Also, we examine the classical representation of conformal symmetry. A representation (π) of a group is defined as mapping from group of symmetries to a set of matrices;

$$\pi : \ G \to M_n(\mathbb{C})$$

.

2.1.5 Classical Field Representations of Conformal Symmetry

Action in clasical field theory is defined as

$$S = \int d^d x \ \mathcal{L}(\Phi, \partial_\mu \Phi). \tag{2.35}$$

Under a symmetry transformation,

$$x \to x' \quad \text{and} \quad \phi(x) \to \phi'(x') \equiv \mathcal{F}[\phi(x)].$$

Such a transformation is called active transformation under which both field and the space-time coordinate change. Let us analyze this transformation with a simple example. The $2D$ rotation in which both coordinates and fields change through an operator O which is just a 2×2 matrix.

$$O = \begin{pmatrix} \cos\theta & \sin\theta \\ -\sin\theta & \cos\theta \end{pmatrix} .$$

So the transformed field can be written as

$$\phi'_a(x) = \sum_b \pi(O)_{ab}\, \phi_b(O^{-1}x) \quad \text{where} \quad \pi(O)_{ab} = [O]_{ab} .$$

This is called the fundamental representation. The action changing under this transformation is

$$S' = \int d^d x \left|\frac{\partial x'}{\partial x}\right| \mathcal{L}\Big(\mathcal{F}[\phi(x)], \frac{\partial x^\nu}{\partial x'^\mu}\partial_\nu \mathcal{F}[\phi(x)]\Big) \quad \text{where} \quad \left|\frac{\partial x'}{\partial x}\right| = \left|det(\frac{\partial x'^\mu}{\partial x^\nu})\right| . \tag{2.36}$$

A theory can be considered as symmetric when equation of motion is invariant under the transformation, in other words;

$$\mathcal{L}' = \mathcal{L} + \partial_\mu N.$$

2.1.6 Infinitesimal Transformations and Generators of Conformal Group

Let us denote ε_a which is a set of infinitesimal parameters. Infinitesimal transformations are

$$x'^\mu \to x^\mu + \varepsilon_a \frac{\delta x^\mu}{\delta \varepsilon_a} \quad \text{and} \quad \phi'(x') = \phi(x) + \varepsilon_a \frac{\delta \mathcal{F}(x)}{\delta \varepsilon_a} .$$

We discard all higher order terms. Generators (G_a) are defined as $\delta_\varepsilon \phi(x) = \phi'(x) - \phi(x) \equiv i\varepsilon_a G_a$. As we can realize that both fields have the same space-time point. In order to understand how generators act, we need to find $\phi'(x)$;

$$\phi'(x') = \phi(x) \; + \varepsilon_a \frac{\delta \mathcal{F}}{\delta \varepsilon_a} = \phi(x') - \varepsilon_a \frac{\delta x^\mu}{\delta \varepsilon_a}\partial_\mu \phi(x') + \varepsilon_a \frac{\delta \mathcal{F}}{\delta \varepsilon_a}(x) . \tag{2.37}$$

Here we use Taylor series expansion. So. the generators may be described as

$$iG_a\phi = \frac{\delta x^\mu}{\delta \varepsilon_a}\,\partial_\mu\phi - \frac{\delta \mathcal{F}}{\delta \varepsilon_a}\,. \tag{2.38}$$

If we assume that the fields are unchanged, $\mathcal{F}[\phi(x)] = \phi(x)$, after the transformation, the infinitesimal generators of conformal group are expressed as follows,

Translation:	$P_\mu = -i\partial_\mu$
Rotation:	$L_{\mu\nu} = i(x_\mu\partial_\nu - x_\nu\partial_\mu)$
Diltation:	$D = -ix^\mu\partial_\mu$
SCT:	$K_\mu = -i(2x_\mu x^\nu\partial_\nu - x^2\partial_\nu).$

We can deduce from here that a field transforming under full conformal group will also transform under subgroup called Poincare group generated by P_μ and $L_{\mu\nu}$,

$$\phi'_a(x) \to \sum_b \pi(\Lambda)_{ab}\;\phi_b(\Lambda^{-1}x)\;.$$

Every conformal transformation is a product of some of these. The Lie algebra of conformal group is constructed by the following commutation relations,

$$[D, P_\mu] = iP_\mu \tag{2.39}$$

$$[D, K_\mu] = -iK_\mu \tag{2.40}$$

$$[K_\mu, P_\mu] = 2i(\eta_{\mu\nu}D - L_{\mu\nu}) \tag{2.41}$$

$$[K_\rho, L_{\mu\nu}] = i(\eta_{\rho\mu}K_\nu - \eta_{\rho\nu}K_\mu) \tag{2.42}$$

$$[P_\rho, L_{\mu\nu}] = i(\eta_{\rho}\mu P_\nu - \eta_{\rho\nu}P_\mu) \tag{2.43}$$

$$[L_{\mu\nu}, L_{\rho\sigma}] = i(\eta_{\nu\rho}L_{\mu\sigma} + \eta_{\mu\sigma} - \eta_{\mu\rho}L_{\nu\sigma} - \eta_{\nu\sigma}L_{\mu\sigma}) \tag{2.44}$$

To write in a more compact form, we can define the following generators

$$J_{\mu\nu} = L_{\mu\nu}, \quad J_{-1,\mu} = \frac{1}{2}(P_\mu - K_\mu), \quad J_{-1,0} = D, \quad J_{0,\mu} = \frac{1}{2}(P_\mu + K_\mu)$$

where $J_{ab} = -J_{ba}$ and $a,\ b \in \{-1, 0, 1...\}$. The commutation relation of the new generators is

$$[J_{ab}, J_{cd}] = i(\eta_{ad}J_{bc} - \eta_{ac}J_{bd} + \eta_{bc}J_{ad} - \eta_{bd}J_{ac})\;. \tag{2.45}$$

For $\mathbb{R}^{d,0}$, $\eta_{ab} = (-1, 1, 1, ...)$. This commutation relation can be recognized immediately, since it is just the relation of the group SO$(d+1, 1)$. This indicate the isomorphism between d dimensional conformal group and SO$(d+1, 1)$.

Moreover, by using the commutation relation $[D, P_\mu] = iP_\mu$, it can be shown that

$$e^{i\alpha D} P^2 e^{-i\alpha D} = e^{2\alpha} P^2 \ . \tag{2.46}$$

If we define a state $P^2 = m^2$, then this relation alludes that the scale symmetry does not allow discrete mass states. Mass can be either continuous or zero.

We now concentrate on a subgroup of the conformal group which fixes the origin. This group includes rotations, dilations and SCTs. The infinitesimal generators are let say G_a forms the sub-algebra. So, suppose we have an infinitesimal transformation $\zeta = e^{i\varepsilon^\alpha G_\alpha}$. The field at origin under this transformation is

$$\phi_a(0) \to \sum_b \pi(e^{i\varepsilon^\alpha G_\alpha})_a \ \phi_b(0).$$

Since ε_α is infinitesimal π can be written as

$$\pi(e^{i\varepsilon^\alpha G_\alpha}) = \pi(I) + i\varepsilon^\alpha \pi(G_\alpha) \quad where \quad G_a = \{K_\mu, D, L_{\mu\nu}\}.$$

Now let us define, $\pi(D) \equiv \tilde{\Delta}$, $\pi(K_\mu) \equiv \kappa_\mu$, $\pi(L_{\mu\nu}) \equiv S_{\mu\nu}$. The representations obey the same rules of Lie algebra. Therefore,

$$\left[\tilde{\Delta}, S_{\mu\nu}\right] = 0, \quad \left[\tilde{\Delta}, \kappa_\mu\right] = -i\kappa_\mu \ . \tag{2.47}$$

The Schur's Lemma states that if a generator commutes with other generators in an irreducible representation ($S_{\mu\nu}$) then the representation must be trivial. In other words, it must be proportional to the identity $\tilde{\Delta} \propto I$. So $\tilde{\Delta} = i\Delta \ I$ where Δ is called the scaling dimension. Instantly we can see that because of the second commutation relation, $\kappa_\mu = 0$. For the rest we will only consider spinless fields. That's why $S_{\mu\nu}$ vanishes also.

Now, let us try to understand how dilation acts on fields. Remember that under infinitesimal dilation, coordinates change to $x \to x + \epsilon x$. When we exponentiate to obtain the full dilation, we get $x \to e^\alpha x \equiv \lambda x$. Under full dilation fields become

$$\phi_a(0) \to (1+i\epsilon\tilde{\Delta})_{ab}(1+i\epsilon\tilde{\Delta})_{ab}....\phi_b(0) = [e^{i\tilde{\Delta}\alpha}]_{ab}\phi_b(0) = [e^{-\Delta\alpha}]_{ab}\phi_b(0) = [\lambda^{-\Delta}]_{ab}\phi_b(0).$$

This is a trivial representation. Hence,

$$\phi_a(0) \to \lambda^{-\Delta}\phi_a(0).$$

Every conformal field has a scaling dimension Δ. So, in general we have

$$\phi'_a(x) = \sum_b \pi(\zeta)_{ab}\ \phi_b(\zeta^{-1}x) = \zeta^{-\Delta}\phi_a(\zeta^{-1}x).$$

This can be written as

$$\phi'_a(x) = \lambda^{-\Delta}\phi_a(\lambda^{-1}x).$$

Let be reminded that under a conformal transformation, $g'_{\mu\nu} = \omega(x)g_{\mu\nu}$ and the jacobian is $\left|\frac{\partial x'}{\partial x}\right| = \omega^{-d/2}$ where d is the space-time dimension. Under a scale transformation $\omega = \lambda^{-2}$ as $x \to \lambda x$. Therefore,

$$\phi'(x') = \left|\frac{\partial x'}{\partial x}\right|^{-\Delta/d}\phi(x). \tag{2.48}$$

The fields that transform like this are called quasi-primary fields. So, we can conclude that fields which are invariant under conformal transformations are quasi-primary fields.

2.1.7 Quantum Conformal Field Theory

We define a set of observable $A_{j,x}$. There is a subset of $\{A_{j,x}|j \in J,\ x \in \mathbb{R}^{p,q}\}$, where J is the index set, described as $\{\hat{\phi}_k(x)|\ k \in K\}$ called quasi-primaries which satisfy the following relation that we already identified in the previous section [1],

$$\hat{\phi_k} \to \left|\frac{\partial x'}{\partial x}\right|^{-d_k/D}\hat{\phi_k}\ . \tag{2.49}$$

Under conformal transformation, there are significant restrictions on the 2-point and 3-point correlation functions. By using (2.49), we can write in general

$$\langle 0|\ \hat{\phi_{k_1}}(x_1)....\hat{\phi_{k_n}}(x_n)\ |0\rangle = \left|\frac{\partial x'_1}{\partial x_1}\right|^{d_{k_1}/D}... \left|\frac{\partial x'_n}{\partial x_n}\right|^{d_{k_n}/D} \langle 0|\ \hat{\phi'_{k_1}}(x'_1)....\hat{\phi'_{k_n}}(x'_n)\ |0\rangle\ . \tag{2.50}$$

The vacuum $|0\rangle$ is assumed to be invariant under conformal transformations.

Translation does not leave the space-time point invariant. However the difference between two space-time points are invariant $(x_i - x_j)$. Under rotation only the lengths or distances ($|x_i - x_j| \equiv r_{ij}$) remains the same. Then, the scale invariance only permits ratios of distances, namely,

$$\frac{r_{ij}}{r_{kl}}.$$

[1] For the rest of the thesis, the scaling dimension is denoted as d and the space-time dimension is denoted as D.

Lastly, if the SCT is imposed, we obtain

$$r'_{ij} = \frac{r_{ij}}{\xi_i^{1/2}\xi_j^{1/2}} \quad \text{where} \quad \xi_i = (1 - 2hx_i + h^2 x_i^2) \, .$$

Therefore the simplest form which is invariant under conformal group is so called cross ratios

$$\frac{r_{jk}r_{lm}}{r_{jl}r_{km}}.$$

Now let us see how the 2-point and 3-point correlation functions behave under conformal transformations. Eq (2.50) tells us that the 2-point correlation function can be written as

$$\big\langle \phi_1(x_1)\phi_2(x_2) \big\rangle = \Big|\frac{\partial x'_1}{\partial x_1}\Big|^{d_1/D} \Big|\frac{\partial x'_2}{\partial x_2}\Big|^{d_2/D} \big\langle \phi'_1(x'_1)\phi'_2(x'_2) \big\rangle \, . \tag{2.51}$$

The jacobian for scale transformation is $\left|\frac{\partial x'}{\partial x}\right| = \lambda^D$ and for SCT, $\left|\frac{\partial x'}{\partial x}\right| = \frac{1}{(1-2hx+h^2x^2)^D}$. Here d_i is the scale dimension. In the view of information that we have discussed on restrictions on conformal transformations, we can say that when the Poincare invariance is imposed, the 2-point correlation function can only depend on distance r_{ij}. Therefore,

$$\big\langle \phi_1(x_1)\phi_2(x_2) \big\rangle = f(r_{12}) \, . \tag{2.52}$$

Under dilation, we know that $f(r_{12}) = \lambda^{d_1+d_2} f(\lambda r_{12})$. This yields

$$f(r_{12}) = \frac{C_{12}}{r_{12}^{d_1+d_2}} \quad \text{where} \quad C_{12} \quad \text{is a constant determined by field renormalization.}$$

Finally, SCT invariance suggests

$$\frac{C_{12}}{r_{12}} = C_{12}\frac{(\xi_1\xi_2)^{(d_1+d_2)/2}}{\xi_1^{d_1}\xi_2^{d_2}} \, .$$

This equality holds only if $d_1 = d_2$. We can now conclude that

$$\big\langle \phi_1(x_1)\phi_2(x_2) \big\rangle = \begin{cases} \dfrac{C_{12}}{r_{12}^{2d}}, & \text{if } \; d = d_1 = d_2 \\ \\ 0, & \text{if } \; d_1 \neq d_2 \end{cases}$$

By the same token, we can determine the 3-point correlation function. After we impose constraints by translation, rotations and dilation the 3-point correlation function is

$$\big\langle \phi_1(x_1)\phi_2(x_2)\phi_3(x_3) \big\rangle = \sum_{a,b,c} \frac{C_{abc}}{r_{12}^a r_{23}^b r_{13}^c} \quad \text{where} \quad a+b+c = d_1+d_2+d_3$$

Then if we apply SCT, we get $a = d_1 + d_2 - d_3$, $b = d_2 + d_3 - d_1$, $c = d_3 + d_1 - d_2$. This results

$$\big\langle \phi_1(x_1)\phi_2(x_2)\phi_3(x_3)\big\rangle = \frac{C_{123}}{r_{12}^{d_1+d_2-d_3} r_{23}^{d_2+d_3-d_1} r_{13}^{d_3+d_1-d_2}}. \tag{2.53}$$

The 2-point and 3-point correlation functions give a very elegant structure. This may also be expected for higher order correlation functions. However, they always have an arbitrary functions which depend on cross ratios. For instance, the four point correlation function restricted by conformal invariance is

$$G^4(x_1, x_2, x_3, x_4) = F\Big(\frac{r_{12}r_{34}}{r_{13}r_{24}}, \frac{r_{13}r_{24}}{r_{23}r_{14}}\Big) \prod_{j<k} r_{jk}^{d/3-(d_j+d_k)} \quad \text{where} \quad d = \sum_j d_j$$

and $F\Big(\frac{r_{12}r_{34}}{r_{13}r_{24}}, \frac{r_{13}r_{24}}{r_{23}r_{14}}\Big)$ is arbitrary.

2.1.8 The 2-point and 3-point Correlation Functions in Momentum Space

In order to find the 2-point correlation function in momentum space we apply Fourier transformation. A correlation function of n fields is

$$\big\langle \phi_1(x_1)....\phi_n(x_n)\big\rangle = \int \frac{d\vec{k}_1...d\vec{k}_{n-1}}{(2\pi)^D...(2\pi)^D}\, \Gamma(\vec{k_1}, ..., \vec{k_n})\, e^{i\sum k_i x_i}. \tag{2.54}$$

Under dilation, $x \to \Lambda x$. The equation (2.54) implies that

$$\Gamma(\vec{k}_1, ..., \vec{k}_n) = \Lambda^{(n-1)D-\sum_{i=1}^n d_i} \Gamma(\Lambda\vec{k}_1, ..., \Lambda\vec{k}_n). \tag{2.55}$$

Also, the 2-point correlation function $\Gamma(\vec{k}_1, -\vec{k}_1) \sim \frac{1}{|\vec{k}|^{D-2d}}$. Even from here we can deduce that the unparticle propagator should be proportional to $\frac{1}{|\vec{k}|^{D-2d}}$. Therefore, in general the 2-point correlation function in momentum space is

$$\Gamma_2(p, d) = A_d\, (p^2)^{d-D/2}. \tag{2.56}$$

For the three point correlation function we have a similar kind of treatment. Again what we will do is simply calculating the Fourier transform of three point correlation function that we have defined in (2.53). It can be written as

$$\Gamma_3(p_1, p_2; d_1, d_2, d_3) = C_{123} \int d^D x_1 d^D x_2\, \frac{1}{|x_{12}|^a |x_1|^b |x_2|^c} e^{-ip_1x_1} e^{-ip_2x_2}. \tag{2.57}$$

where $x_{12} \equiv x_1 - x_2$.

In the next step, by inserting the completeness relation

$$1 = \int d^D z \delta(z - (x_1 - x_2)) = \int \frac{d^D q}{(2\pi)^D} d^D z \, e^{-iq(z-(x_1-x_2))}$$

we can write

$$\begin{aligned}
\Gamma_3 &= \\
&= C_{123} \int \frac{d^D q}{(2\pi)^D} d^D z d^D x_1 d^D x_2 \frac{1}{|z|^a |x_1|^b |x_2|^c} \, e^{-ip_1 x_1} e^{-ip_2 x_2} e^{-iq(z-(x_1-x_2))} \\
&= C_{123} \int \frac{d^D q}{(2\pi)^D} d^D z d^D x_1 d^D x_2 \frac{1}{|z|^a |x_1|^b |x_2|^c} \, e^{-ix_1(p_1-q)} e^{-ix_2(p_2+q)} e^{-iqz}
\end{aligned} \tag{2.58}$$

Now, three position space integration gives three 2-point correlation functions that we have described in (2.56) with scaling dimensions $a/2, b/2, c/2$. Considering that constants are absorbed by C_{123}, the 3-point correlation function in momentum space becomes a loop integral

$$\Gamma_3(p_1, p_2; d_1, d_2, d_3) = C_{123} \int \frac{d^D q}{(2\pi)^D} \Gamma_2(q; a/2) \Gamma_2(p_1 - q; b/2) \Gamma_2(p_2 + q; c/2) \tag{2.59}$$

This integral can be calculated using the trick called Feynman parameters;

$$\frac{1}{C_1^{m_1} .... C_n^{m_n}} = \int_0^1 \prod_{k=1}^{n} dx_k \delta(\sum x_i - 1) \frac{\prod x_i^{m_i - 1}}{(\sum x_i C_i)^{\sum m_i}} \frac{\Gamma(\sum m_i)}{\prod \Gamma(m_i)}.$$

In our situation $n = 3$ and

$$\begin{aligned}
C_1 &= q^2 & m_1 &= D/2 - a/2 \\
C_2 &= (p_1 - q)^2 & m_2 &= D/2 - b/2 \\
C_3 &= (p_2 + q)^2 & m_3 &= D/2 - c/2.
\end{aligned}$$

The term in the denominator by using the change of variables can be rewritten as

$$\sum C_i x_i = q^2 x_1 + (p_1 - q)^2 x_2 + (p_2 + q)^2 x_3 = l^2 + s\Omega$$

where

$$s = (p_1 + p_2)^2$$

$$l = q + x_3 p_2 - x_2 p_1$$

$$\Omega = x_1 x_2 \frac{p_2^2}{s} + x_2 x_3 + x_1 x_3 \frac{p_1^2}{s}.$$

Hence, the integral turns out to be

$$\Gamma_3(p_1,p_2;d_1,d_2,d_3) = C_{123}\int \frac{d^Dq}{(2\pi)^D}dx_1dx_2dx_3\ \delta(x_1+x_2+x_3-1) \times \frac{x_1^{m_1-1}x_2^{m_2-1}x_3^{m_3-1}}{(l^2+s\Omega)^{m_1+m_2+m_3}}\cdot\frac{\Gamma(m_1+m_2+m_3)}{\Gamma(m_1)\Gamma(m_2)\Gamma(m_3)}.$$

Now, let us change the integration variable from q to ℓ. The Jacobian is identity i.e., $d\ell = dq$. By using the following result

$$\int \frac{d^D\ell}{(2\pi)^d}\frac{1}{(l^2+s\Omega)^n} = \frac{1}{(4\pi)^{D/2}}.\frac{\Gamma(n-D/2)}{\Gamma(n)}.\Big(\frac{1}{s\Omega}\Big)^{n-D/2}$$

where $n = 3D/2 - 1/2(D_1+D_2+D_3)$, we can finally have

$$\Gamma_3(p_1,p_2;d_1,d_2,d_3) = C_{123}G_{123} \times \Big(\frac{1}{s}\Big)^{D-1/2(d_1)+d_2+d_3}\int dx_1dx_2dx_3.\delta(x_1+x_2+x_3-1) \times \Big(\frac{1}{\Omega}\Big)^{D-1/2(d_1+d_2+d_3)} x_1^{m_1-1}x_2^{m_2-1}x_3^{m_3-1}.$$

where

$$G_{123} = \frac{\Gamma(D-1/2(d_1+d_2+d_3))}{(4\pi)^{D/2}\Gamma(m_1)\Gamma(m_2)\Gamma(m_3)}\ .$$

Let us consider the Minkowski space ($D=4$) and let us assume that all the fields have the same scaling dimension d. Then $m_i = 2-d/2 \quad$ where $i=1,2,3$. Eventually, the 3-point correlation function becomes

$$\Gamma_3(p_1,p_2;d) = A_d\Big(\frac{1}{s}\Big)^{4-3d/2}F\Big(\frac{p_1^2}{s},\frac{p_2^2}{s}\Big) \tag{2.60}$$

where

$$F\Big(\frac{p_1^2}{s},\frac{p_2^2}{s}\Big) = \frac{\Gamma(4-3d/2)}{\Gamma(2-d/2)^3}\frac{1}{(4\pi)^2}\int dx_1dx_2dx_3\delta(x_1+x_2+x_3-1) \times \frac{1}{(\Omega)^{4-3d/2}}.(x_1x_2x_3)^{1-d/2}.$$

2.1.9 Unitarity

In his paper in 1977 [27] Mack classified all the unitarity irreducible representations of conformal group. They are tagged by scale dimension d and irreducible representation of Lorentz group (j_1,j_2) . Totally there are five representations. The difference

between them are determined by Poincare content, mass and spin. The unitarity condition restricts the scale dimension d. It brings a general lower bound on scaling dimension of operators in CFT:

$$d \geq j_1 + j_2 + 2 - \delta_{j_1,j_2,0}$$

Therefore,

$$d_s \geq 1$$
$$d_f \geq 3/2$$
$$d_v \geq 3$$

where d_s, d_f, d_v scaling dimensions of scalar, fermionic, and vector operators, respectively.

2.2 Effective Field Theory

The ultimate aim of physicists is to describe all physics with an one single theory. Whenever we reach a new energy scale, we always encounter with new physical phenomena. Moreover it is getting harder to make computations as distances become smaller, thus energy is getting higher. Therefore it is convenient to only study physics with degrees of freedom which are relevant to the particular scale. So, in each different scale there is an appropriate description for relevant physics.

Effective Field Theory (EFT) is an approximation method to determine low-energy physics. By low-energy we mean that it is low with respect to a built-in scale Λ. The idea of EFT is to describe physical processes at energies at a given scale E with an accuracy ϵ which can be determined by orders of E/Λ.

2.2.1 Relevant, Irrelevant, Marginal Couplings

Let us assume that the ϕ^4 field theory with interaction terms included as an EFT. So, the action in D dimensions can be written as

$$S = \int d^D x \left(\frac{1}{2} \partial_\nu \phi \partial^\nu \phi - \frac{1}{2} m^2 \phi^2 - \frac{\lambda}{4!} \phi^4 - \frac{\tau}{6!} \phi^6 \right) . \tag{2.61}$$

By using the dimension analysis, we may determine the mass dimension of each parameter. Since the action should be dimensionless, the dimension of parameters can be defined as

$$[\phi] = \frac{D-2}{2} \,, \tag{2.62}$$

$$[m^2] = 2 \,, \tag{2.63}$$

$$[\lambda] = 4 - D \,, \tag{2.64}$$

$$[\tau] = 6 - 2D \,. \tag{2.65}$$

Now, in order to study correlation functions at long distances or small momentum, we may rescale coordinates $x^\nu \to s x'^\nu$ where x' is fixed and $s \to \infty$. To keep the kinetic term intact, we may define

$$\phi'(x') = s^{(D-2)/2}\phi(x) \tag{2.66}$$

and therefore the correlation function becomes

$$\big\langle \phi(x_1)....\phi(x_N) \big\rangle = s^{N(D-2)/2} \big\langle \phi'(x'_1)....\phi'(x'_N) \big\rangle. \tag{2.67}$$

Then the transformed action can be written as

$$S' = \int d^D x' \left(\frac{1}{2}\partial'_\nu \phi' \partial'^\nu \phi' - \frac{1}{2} m^2 \phi'^2 - \frac{\lambda}{4!}\phi'^4 - \frac{\tau}{6!}\phi'^6 \right). \tag{2.68}$$

The rescaled mass term in S' is $s^2 m^2$. So, in the limit of very large s values the importance of the coupling term m^2 gets more significant. This is called relevant coupling and ϕ^2 operator is identified as relevant operator. The term including the ϕ^6 term becomes very small as s has large values. Therefore τ becomes less and less important. This coupling is called irrelevant. After we rescale the action, the ϕ^4 term remains same. Hence, ϕ^4 is called marginal operator and λ is equally important and known as marginal coupling. Therefore, in general we may write

$$\text{Relevant :} \quad dim < D \,, \tag{2.69}$$

$$\text{Marginal :} \quad dim = D \,, \tag{2.70}$$

$$\text{Irrelevant :} \quad dim > D. \tag{2.71}$$

We can relate mass dimension of parameters with a new scale Λ of new physics

$$m^2 \sim \Lambda^2, \;\; \lambda \sim \Lambda, \;\; \tau \sim \Lambda^{-2} \tag{2.72}$$

and we can do power counting in this high energy scale Λ.

2.2.2 Effective Lagrangian

In general a renormalizable theory includes only the operators with space-time dimension $[O] < D$. In a renormalizable theory divergences can be absorbed by a finite amount of counter-terms. However if it is not the case, then an infinite number of counter-terms are needed. Because of that there will be infinite number of unknown parameters. As a aresult of this, theory looses its predictive power.

On the other hand, an effective Lagrangian includes infinite number of interaction terms which satisfy the underlying symmetry

$$\mathcal{L}_{eff} = \mathcal{L}_{\leq D} + \mathcal{L}_{D+1} + \mathcal{L}_{D+2} + ... \tag{2.73}$$

where $\mathcal{L}_{\leq D}$ is the renormalizable Lagrangian and in the terms with $[O] > D + a$ where $a > 0$ renormalizability is violated. We need to know all of these terms to get full theory. We still require infinite number of counter-terms. However, the matrix elements of these operators are proportional to $\langle \mathcal{L}_{D+n} \rangle \sim (E/\Lambda)^n$ where Λ is some mass scale of high energies and E, the energy of given theory can be defined as $E = \Lambda/s$ where $s > 0$.

Therefore, the effective Lagrangian can be renormalized order by order in $1/\ \Lambda^n$ or $1/s^n$. We can calculate with an error of $1/s$ by maintaining only $\mathcal{L}_{\leq D}$. Moreover we can extend this. In order to make calculations with an error $1/s^{n+1}$, we need to keep terms up to $\mathcal{L}_{D+n}$. In other words, to include all corrections up to $1/s^n$, we need to include all operators up to order $[O] \leq D + n$. So, we will have a finite number of parameters with a given accuracy. Hence, the theory still have the predictive power.

We can realize that as $s \to \infty$, all terms except which have operators with $[O] \leq D$ vanishes. Therefore we can do computations with no error in this case.

2.2.3 Weak Interactions of Low Energies

The basic and yet powerful example of an EFT is Fermi theory of weak interactions. The underlying renormalizable $SU(2) \times U(1)$ electroweak theory can be described at low energies by Fermi Theory at tree level.

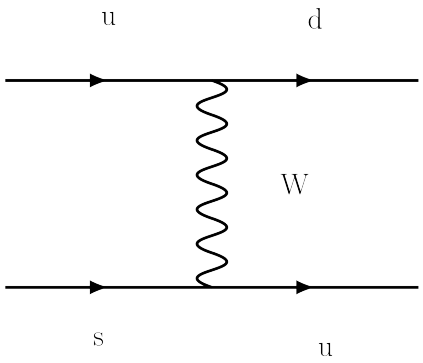

Figure 2.1: W exchange diagram for weak interaction.

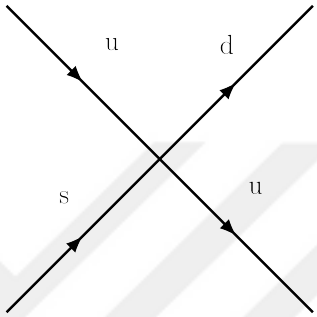

Figure 2.2: Fermi four point effective diagram.

We can consider quark-quark scattering process $u + s \to d + u$ through the exchange of W-boson between two left-handed fermionic currents whose Feynman diagram is given in Fig. (2.1)

$$V^{\nu} = \frac{-i\lambda}{\sqrt{2}}\, V_{ab}\, \overline{q_i}\, \gamma^{\nu} P_L\, q_j. \tag{2.74}$$

Here V_{ab} is the CKM-matrix and P_L is the left-handed projection operator. If we do not take loop corrections into account, the matrix element of the process $u+s \to d+u$ can be described as

$$\frac{\lambda^2}{2} V_{us} V_{ud}^{*} (\bar{u}\gamma^{\alpha} P_L s)(\bar{d}\gamma_{\alpha} P_L u)\Big(\frac{-i}{q^2 - M_W^2}\Big)\,. \tag{2.75}$$

Here $u,\ d,\ s$ are spinor fields. At very low energies where the transferred momentum q is small compared to M_W, by applying the Taylor series expansion the propagator can be written as

$$\frac{1}{q^2 - M_W^2} = \frac{-1}{M_W^2}\Big(1 + \frac{q^2}{M_W^2} + \frac{q^4}{M_W^4}\Big)\,. \tag{2.76}$$

Therefore, at low energies the effective interaction term is

$$\mathcal{L} = \frac{-4G_F}{\sqrt{2}}\, V_{us}\, V_{ud}^{*}\, (\bar{u}\gamma^{\alpha} p_L s)(\bar{d}\gamma_{\alpha} P_L u) + \mathcal{O}\Big(\frac{1}{M_w^4}\Big) \tag{2.77}$$

which is described by local four-fermion vertex given in Fig. (2.2). So, the renormalizable electroweak interaction can be written in terms of QED and effective Lagrangian term with a correction up to order $\mathcal{O}(1/M_W)^4$. We can also see that the dimension of operator in effective Lagrangian term is six. Hence, as we have discussed earlier, this operator can be considered as irrelevant.

Even if we may have infinitely many terms, we can still describe interaction with a finite number of parameters with an accuracy (p^2/M_W^2) by neglecting higher order terms. It is legitimate to do that since higher order contributions will be suppressed by the negative powers of M_W. For further readings, see [28, 29].

2.3 Banks-Zaks Fixed Point

Quantum Field Theory (QFT) generically can be considered as a study of Renormalization Group (RG) flows [30], which is the way to determine how theory evolves from high energy (UV) to low energies (IR). There are so-called three possible IR phases. The first one is a theory with a mass gap. The second is a theory of massless particles in the IR. QED is a trivial example of this theory. The last one which will be the topic of discussion in this section is a scale invariant theory with a continuous mass spectrum. Now, lets concentrate on the beta function which is formed by two loops quantum corrections

$$\beta = b_0 g^3 + b_1 g^5 + \mathcal{O}\left(g^7\right) . \tag{2.78}$$

The non-trivial roots of β-function, say g^*, i.e., $\beta(g^*) = 0$ are called fixed points. This theory possesses conformally symmetric properties. For fixed points to be weakly coupled ($g^{*2} \ll 1$), b_0 should be negative as well as $b_1 > 0$. Now let us consider specifically

$$b_0 = -\frac{\beta_0}{16\pi^2} \quad \text{and} \quad b_1 = -\frac{\beta_1}{(16\pi^2)^2}$$

where

$$\beta_0 = \frac{11}{3}N_c - \frac{2}{3}N_f \quad \text{and} \quad \beta_1 = \Big[\frac{34}{3}N_c^2 - \frac{1}{2}N_f\Big(\frac{2N_c^2-1}{N_c} + \frac{20}{3}N_c\Big)\Big].$$

Here N_c is the number of colors and N_f is the number of fermion flavors. If $N_c, N_f \gg 1$, we have $\beta_0 \sim \mathcal{O}(1)$ (Near cancellation) and $\beta_1 \sim \mathcal{O}(N_c^2)$. Then let us focus on

eqn (2.78). It vanishes if

$$g^{*2} = -\frac{b_0}{b_1} \sim \mathcal{O}\Big(\frac{16\pi^2}{N_c^2}\Big).$$

Moreover, lets define λ^* by

$$\lambda^* = \frac{N_c g^{*2}}{16\pi^2} \sim \mathcal{O}(1/N_c)\ .$$

The effects coming from higher order are suppressed by the powers of N_c. Therefore we are still in perturbative regime. This fixed point λ^* is the so called Banks-Zaks (BZ) fixed point [31]. Remember that $b_0 < 0$ and $b_1 > 0$. Hence the values N_c and N_f are needed to satisfy the following conditions;

$$N_f < \frac{11}{2}N_c \quad \text{and} \quad N_f > \frac{34N_c^3}{13N_c^2 - 3}\ .$$

If we put them together

$$\frac{34N_c^3}{13N_c^2 - 3} < N_f < \frac{11}{2}N_c\ .$$

This is called the "conformal window" in which BZ-fixed point appears. The physics at IR fixed point is not similar to QFT. Through the flowing, any operator gains an anomalous dimension which freezes at the fixed point. The anomalous dimension of $\psi\bar{\psi}$ operator is

$$\gamma(g_*) = \frac{-g_*^2}{2\pi^2}.$$

Therefore the scale dimension of operators can have non- integer dimensions. This causes that spectral density becomes continuous and there is not any well-defined particles.

In the next chapter, this idea will be realized in the context of so-called unparticle stuff.

CHAPTER 3

UNPARTICLE PHYSICS

In this chapter, we begin with the basics of the unparticle stuff. After that we define the two most important features of unparticle, namely the phase space and propagators. Then we try to understand the couplings between standard model and unparticle stuff and we are going to determine Feynman rules for various interactions. As an example we consider the process $t \to uU$ and assume the unparticle does not decay within the detector so that it appears to be as a missing energy.

3.1 The Model

The scheme is as follows. At a very high scale a Banks-Zaks (BZ) type hidden sector interacts with Standard Model (SM) via the messenger field with large mass M_U. SM fields and BZ fields do not couple directly since both of them carry different gauge group charges etc. The messenger field is assumed to carry properties allowing it to couple both fields. Below the energy M_U, by using the effective field theory one can integrate out the heavy scale and get a generic effective Lagrangian of the form

$$\mathcal{L}_{int}^{eff} = \frac{C_U}{M_U^{d_{SM}+d_{BZ}-4}} O_{SM} O_{BZ} \ . \tag{3.1}$$

The non-renormalizable couplings of the SM and BZ fields be suppressed by M_U. The mass dimension of SM and BZ fields are d_{SM} and d_{BZ} respectively and O_{SM}, O_{BZ} are local operators. As we run into low energies, at a cut off scale Λ scale invariance emerges. As in the case of massless non-abelian gauge groups, the renormalizable couplings of BZ fields cause the so-called dimensional transmutation

$$C_U \to \Lambda^{d_{BZ}-d_U} C_U.$$

which means that our otherwise dimensionless couplings gain mass dimension. Below the scale Λ, because of the matching condition of EFT, BZ operators match onto unparticle operators O_U. So finally the interaction term turns into

$$\mathcal{L}_{int}^{eff} = C_U \frac{\Lambda^{d_{BZ}-d_U}}{M_U^{d_{SM}+d_{BZ}-4}} O_{SM} O_U. \tag{3.2}$$

where d_U is the scaling dimension of unparticle operator O_U. We can define

$$\Lambda_U^{d_U+d_{SM}-4} \equiv \frac{M_U^{d_{SM}+d_{BZ}-4}}{\Lambda^{d_{BZ}-d_U}}. \tag{3.3}$$

So, finally we may write

$$\mathcal{L}_{int}^{eff} = C_U \frac{1}{\Lambda_U^{d_U+d_{SM}-4}} O_{SM} O_U \tag{3.4}$$

As we understood in previous sections, the leading contributions comes from lowest order operators. Hence, we consider the unparticle operator as such. Also we can say that operators with different mass dimension will couple with different strengths. So the Λ value is not unique or comparable.

If M_U is large enough, unparticles cannot couple strongly to ordinary matter. Therefore it can appear only in high energies, thus at colliders. Two useful properties of using EFT approach are that BZ decouples from ordinary matter at low energies and that the IR scale invariance remains intact.

3.2 The Phase Space of Unparticle

As we have discussed in the section 1.3, the conformal symmetry restricts two-point correlation function. Let us consider an unparticle operator O_U. Then we can write the two-point correlation function in vacuum from x to x' as

$$G \equiv \langle 0 | \, O_U(x) O_U^{\dagger}(x') \, | 0 \rangle \, . \tag{3.5}$$

We normalize the state at vacuum as

$$\langle 0 | \, O_U(x) \, | 0 \rangle = 0. \tag{3.6}$$

By using the translation operator we can define the unparticle operator;

$$O_U(x) = e^{ipx} O_U e^{-ipx}. \tag{3.7}$$

where p^μ is the the energy-momentum operator and $p^\mu |0\rangle = 0$. So, the two-point correlation function becomes

$$G = \langle 0| O_U(0) e^{-ip(x-x')} O_U^\dagger(0) |0\rangle . \tag{3.8}$$

Next we can insert the following completeness relation

$$\int |\lambda\rangle \langle\lambda| \, d\lambda = 1$$

where λ is an eigenstate of energy-momentum operator i.e. $p^\mu |\lambda\rangle = p^\mu_\lambda |\lambda\rangle$. Therefore we have

$$G = \int d\lambda e^{-ip_\lambda(x-x')} \langle 0| O_U(0) |\lambda\rangle \langle\lambda| O_U^\dagger(0) |0\rangle \tag{3.9}$$

$$= \int d\lambda e^{-ip_\lambda(x-x')} |\langle 0| O_U(0) |\lambda\rangle|^2 \tag{3.10}$$

We exclude vacuum state $\langle 0| O_U(0) |0\rangle$. We can only have positive energies $p^0 > 0$ as if there would be otherwise negative energies and the ground state would not be stable. Moreover if we also insert the effective description of the following identity [32]

$$\int_0^\infty ds \int d^4p \delta(p^2 - s)\theta(p^0)\delta^4(p - p_\lambda) = 1, \tag{3.11}$$

we obtain

$$G = \int_0^\infty ds \int d^4p \delta(p^2 - s)\theta(p^0) e^{-ip_\lambda(x-x')} \int d\lambda \delta^4(p - p_\lambda) |\langle 0| O_U(0) |\lambda\rangle|^2 . \tag{3.12}$$

Now, we can define the phase space of unparticle as

$$\rho_U(p^2) \equiv (2\pi)^4 \int d\lambda \delta^4(p - p_\lambda) |\langle 0| O_U(0) |\lambda\rangle|^2. \tag{3.13}$$

Hence, finally the two-point correlation function can be written as

$$\langle 0| O_U(x) O_U^\dagger(x') |0\rangle = \frac{1}{(2\pi)} \int_0^\infty \rho_U(s) ds \xi(x - x'; s) \tag{3.14}$$

where

$$\xi(x - x'; s) = \int \frac{d^4p}{(2\pi)^3} \theta(p^0) e^{-ip(x-x')} \delta(s - p^2) .$$

It can also be described as follows

$$G = \langle 0| O_U(x) O_U^\dagger(x') |0\rangle = \int \frac{d^4p}{(2\pi)^4} e^{-ip(x-x')} \rho_U(p^2). \tag{3.15}$$

Remember from section 1.3.1, in momentum space the two-point unordered correlation function of conformal operators is

$$\langle 0|\, O_U(x) O_U^\dagger(x')\, |0\rangle = \int \frac{d^4p}{(2\pi)^4} e^{-ip(x-x')} \Gamma_2(p) \tag{3.16}$$

where Γ_2 is proportional to $(p^2)^{d_U-2}$. Therefore it is obvious from eq (3.15) that $\rho_U(p^2) \sim (p^2)^{d_U-2}$. The phase space is positive and we want unparticle to be non-tachyonic. With these restrictions the phase space of unparticle stuff can be describe as

$$\rho_U(p^2) = A_{d_U} \theta(p^0)\theta(p^2)(p^2)^{d_U-2} \tag{3.17}$$

where $A_{d_U} > 0$ is the normalization constant needed to be determined.

The phase space of n massless particles has a very similar description;

$$(2\pi)^4 \int \delta^4\Big(p - \sum_{j=1}^{n} p_j\Big) \prod_{j=1}^{n} \delta(p_j^2)\delta(p_j^0) \frac{d^4p}{(2\pi)^4} = A_n \theta(p^0)\theta(p^2)(p^2)^{n-2} \tag{3.18}$$

where

$$A_n = \frac{16\pi^{5/2}}{(2\pi)^{2n}} . \frac{\Gamma(n+1/2)}{\Gamma(n-1)\Gamma(2n)} .$$

Let us demand that $A_{d_U} \to A_n$. In other words we identify A_{d_U} as

$$A_{d_U} = \frac{16\pi^{5/2}}{(2\pi)^{2d_U}} . \frac{\Gamma(d_U+1/2)}{\Gamma(d_U-1)\Gamma(2d_U)} .$$

This is reasonable since even if A_{d_U} has a different description, we may still change it to the desired definition and remnants can be absorbed by the constant C_U. In conclusion, unparticle seems like d_U number of particles. Here since the scaling dimension may take non-integral values, we have a structure that cannot be explained in terms of particle physics. That is why we have this special notion called unparticle stuff.

3.3 An example : $t \to uU$

In order to understand unparticle in a more realistic case, we may consider the decay of top quark to up quark and unparticle of scaling dimension d_U, $t \to uU$ as depicted in figure 3.1.

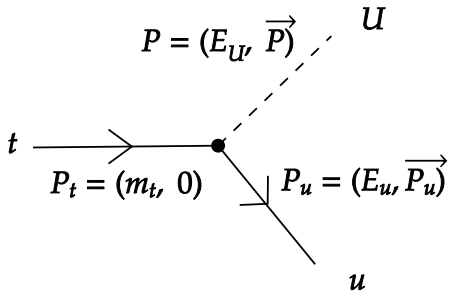

Figure 3.1: The Feynman diagram for $t \to uU$ process

The simplest interaction that can be written is

$$\frac{i\lambda}{\Lambda^{d_U}}\bar{u}\gamma_\mu(1-\gamma_5)t\,\partial^\mu O_U \; + h.o.t \tag{3.19}$$

We can define the amplitude of the diagram as

$$\mathcal{M} = \frac{i\lambda}{\Lambda^{d_U}}\bar{u}(P_u)\gamma_\mu(1-\gamma_5)t(P_t)P^\mu \tag{3.20}$$

Thus, the adjoint of the matrix element is

$$\mathcal{M}^\dagger = \frac{-i\lambda}{\Lambda^{d_U}}P^\nu\bar{t}(1+\gamma_5)\gamma_\nu u \tag{3.21}$$

Hence, the square of the average amplitude can be written as

$$\overline{|\mathcal{M}|^2} = \frac{\lambda^2}{\Lambda^{2d_U}}P^\mu P^\nu tr\{\not{P}_u\gamma_\mu(1-\gamma_5)(\not{P}_t + m_t)(1+\gamma_5)\gamma_\nu\} \tag{3.22}$$

$$= \frac{\lambda^2}{\Lambda^{2d_U}}P^\mu P^\nu tr\{\not{P}_u\gamma_\mu(1-\gamma_5)\not{P}_t\gamma_\nu\} \tag{3.23}$$

$$= \frac{\lambda^2}{\Lambda^{2d_U}}P^\mu P^\nu \Big[tr\{\not{P}_u\gamma_\mu\not{P}_t\gamma_\nu\} - tr\{\not{P}_u\gamma_\mu\gamma_5\not{P}_t\gamma_\nu\}\Big] \tag{3.24}$$

So,

$$\overline{|\mathcal{M}|^2} = \frac{4\lambda^2}{\Lambda^{2d_U}}P^\mu.P^\nu\big[P_u^\alpha P_t^\beta(g_{\alpha\mu}g_{\beta\nu} + g_{\alpha\nu}g_{\beta\mu} - g_{\alpha\beta}g_{\mu\nu})\big] \tag{3.25}$$

$$= \frac{4\lambda^2}{\Lambda^{2d_U}}\big[2(P.P_u)(P.P_t) - (P_u.P_t)P^2\big] \tag{3.26}$$

In the center of mass frame $P = P_t - P_u$, if we neglect the mass of the up quark, we may have

$$P.P_u = P_t.P_u \tag{3.27}$$

$$P.P_t = m_t^2 - P_u.P_t \tag{3.28}$$

$$P^2 = m_t^2 - 2P_u.P_t. \tag{3.29}$$

Therefore the amplitude square can further be written as

$$\overline{|\mathcal{M}|^2} = \frac{4\lambda^2}{\Lambda^{2d_U}}(P_u \cdot P_t)m_t^2 \tag{3.30}$$

In general the decay rate in particle physics is defined as

$$d\Gamma = \frac{\overline{|\mathcal{M}|^2}}{2m_t} d\phi(P_t). \tag{3.31}$$

where

$$d\phi(P_t) = \int (2\pi)^4 \delta^4(P_t - P_u - P) d\phi(P_u) \frac{d^4P_u}{(2\pi)^4} d\phi(P) \frac{d^4(P)}{(2\pi)^4} \tag{3.32}$$

is the Lorentz invariant phase space. Also,

$$d\phi(P) = A_{d_U}\theta(P^0)\theta(P^2)(P^2)^{d_U-2} \tag{3.33}$$

$$d\phi(P_u) = 2\pi\theta(P_u^0)\delta(P_u^2) \tag{3.34}$$

Therefore the decay rate is rewritten as,

$$\begin{aligned}
\int d\Gamma &= \frac{2\lambda^2}{\Lambda^{2d_U}} A_{d_U} m_t \int (P_u.P_t)(2\pi)^4 \delta^4(P_t - P_u - P)\, \frac{d^4P_u}{(2\pi)^4}\, [2\pi\theta(P_u^0)\delta(P_u)^2] \\
&\times \frac{d^4P}{(2\pi)^4} \big[\theta(P^0)\theta(P^2)(P^2)^{d_U-2}\big] \\
&= \frac{2\lambda^2}{\Lambda^{2d_U}} A_{d_U} m_t \int (P_u \cdot P_t) \frac{d^4P_u}{(2\pi)^3} \big[\theta(P_u^0)\delta(P_u^2)\big] \\
&\times \theta(P_t^0 - P_u^0)\theta\big((P_t - P_u)^2\big)(P_t - P_u)^{2(d_U-2)} \\
&= \frac{2\lambda^2}{\Lambda^{2d_U}} A_{d_U} m_t \int \frac{d^3\vec{P}_u}{(2\pi)^3}\, dP_u^0\, \theta(P_u^0)\delta(P_u^{0^2} - \vec{P}_u^2)(P_u^0 P_t^0) \\
&\times \theta(P_t^0 - P_u^0)\, \theta\big(P_t - P_u)^2\big)[m_t^2 - 2P_u^0 P_t^0]^{d_U-2}
\end{aligned}$$

Define $|\vec{P}_u| \equiv r$ and $P_u^0 \equiv E_u$. Then $d^3\vec{P}_u = |\vec{P}_u|^2 d|\vec{P}_u|\, d\Omega = r^2 dr d\Omega$. So, the decay rate becomes

$$\int d\Gamma = \frac{2\lambda^2}{\Lambda^{2d_U}} \frac{A_{d_U} m_t}{(2\pi)^3} \int r^2 dr d\Omega\, dE_u\, \delta(E_u^2 - r^2)\, (E_u m_t) \tag{3.35}$$

$$\times\, \theta(E_u)\theta(m_t - E_u)\theta(m_t^2 - 2m_t E_u)\big[m_t^2 - 2E_u m_t\big]^{d_U-2} \tag{3.36}$$

Integrate over r

$$I' = \int r^2 dr \; E_u \delta(E_u^2 - r^2). \tag{3.37}$$

Define $\beta \equiv r^2$ and then

$$\int \frac{\sqrt{\beta}}{2} d\beta \; E_u \delta(E_u^2 - \beta) = \frac{E_u^2}{2} \; . \tag{3.38}$$

Then we may obtain

$$\int d\Gamma = \frac{2\lambda^2}{\Lambda^{2d_U}} \frac{A_{d_U}.m_t}{(2\pi)^2} \int dE_u E_u^2 \theta(E_u)\theta(m_t - E_u) \tag{3.39}$$

$$\times \; \theta(m_t^2 - 2m_t E_u)\left[m_t^2 - 2E_u m_t\right]^{d_U - 2} \tag{3.40}$$

Now, $\theta(E_u) \to E_u > 0$, $\theta(m_t - E_u) \to m_t > E_u > 0$, $\theta(m_t^2 - 2m_t E_u) \to m_t > 2E_u > 0$. Thus,

$$\int d\Gamma = \frac{2\lambda^2}{\Lambda^{2d_U}} \frac{A_{d_U} m_t}{(2\pi)^2} \int dE_u E_u^2 \frac{\theta(m_t - 2E_u)}{\left[m_t^2 - 2E_u m_t\right]^{2-d_U}} \tag{3.41}$$

and

$$\frac{d\Gamma}{dE_u} = \frac{2\lambda^2}{\Lambda^{2d_U}} \frac{A_{d_U} m_t}{(2\pi)^2} \; E_u^2 \; \frac{\theta(m_t - 2E_u)}{\left[m_t^2 - 2E_u m_t\right]^{2-d_U}} \tag{3.42}$$

The energy spectrum is continuous in $0 \leq E_u \leq m_t/2$. As $d_U \to 1^+$, the spectrum becomes peaked at $E_u = m_t/2$, it reproduce the kinematics of two-body decay as expected.

3.4 The Unparticle Propagator

In this thesis we study the virtual effects of scalar unparticle stuff. In order to do that we ought to describe the unparticle propagator. We will start our discussion with unordered two-point correlation function that we have found in the previous section;

$$\langle 0| \, O_U(x) O_U^\dagger(x') \, |0\rangle = \frac{1}{(2\pi)} \int_0^\infty ds \rho_U(s) \xi(x - x'; s) \tag{3.43}$$

where $\rho(s) = A_{d_U}(s^2)^{d_U - 2}$. The time ordered two point correlation function

$$\langle 0| \, T\{O_U(x) O_U^\dagger(x')\} \, |0\rangle \equiv \theta(x^0 - x'^0) \, \langle 0| \, O_U(x) O_U^\dagger(x') \, |0\rangle + \theta(x'^0 - x^0) \, \langle 0| \, O_U^\dagger(x') O_U(x) \, |0\rangle$$

then can be written as

$$\langle 0| \, T\{O_U(x) O_U^\dagger(x')\} \, |0\rangle = \frac{1}{(2\pi)} \int_0^\infty ds \rho_U(s) \xi^+(x - x'; s) \tag{3.44}$$

where

$$\xi^{+}(x-x';s)=\int\frac{d^4p}{(2\pi)^4}\,\frac{e^{-ip(x-x')}}{p^2-s+i\epsilon}$$

The Fourier transform of this gives us the unparticle propagator

$$\Delta_F(p^2)\equiv\int_0^\infty d^4x e^{ipx}\,\langle 0|\,T\{O_U(x)O_U^{\dagger}(0)\}\,|0\rangle=\frac{1}{(2\pi)}\int_0^\infty\frac{ds\rho(s)}{p^2-s+i\epsilon}\tag{3.45}$$

where we assume $x'=0$ just for convenience.

Before calculating the integral, we can consider that the propagator should be proportional to $(-p^2)^{d_U-2}$ which is a complex function. Let us constraint the polar angle of this function to $(-\pi,\pi]$. The complex function is real for $p^2<0$. However it requires a branch cut for positive values of the momentum. In the light of such information, if we perform this integral we get

$$\Delta_F(p^2)=\frac{A_{d_U}}{2\sin(d_U\pi)}(-p^2-i\epsilon)^{d_U-2}\tag{3.46}$$

where

$$(-p^2-i\epsilon)^{d_U-2}=\begin{cases}(p^2)^{d_U-2} & \text{if } p^2<0\\ (p^2)^{d_U-2}e^{-id_U\pi} & \text{if } p^2>0\end{cases}$$

. This unexpected result may make sense because of the following two reasons. First one is that in the limit $d_U\to 1^+$, $\Delta_F(p^2)\to 1/p^2$. Hence, we recover the usual form for massless particles as it should be. The second reason is that the non-trivial phases along the cut in the Lehmann-Kallen formula help us to reproduce the scale invariance;

$$\begin{aligned}\Delta_F(p^2)&=\frac{iA_{d_U}}{2\sin(d_U\pi)}(p^2)^{d_U-2}\big((-1-i\epsilon)^{d_U-2}-(-1+i\epsilon)^{d_U-2}\big)\\&=\frac{iA_{d_U}}{2\sin(d_U\pi)}(p^2)^{d_U-2}\big(e^{-i(d_U-2)\pi}-e^{i(d_U-2)\pi}\big)\\&=A_{d_U}(p^2)^{d_U-2}\end{aligned}$$

This is the satisfactory result that we have constructed in section (1.3). Remember from unitary condition that for scalar unparticle $d_U>1$. We may have singularity in propagator because of the denominator term $\sin(d_U\pi)$. The integer values may lead to multi-particle cuts which restricts us to describe single unparticle field. Therefore we will just take $1<d_U<2$ into consideration. The phases are also important because unique interference effects can be produced. Moreover $(-p^2)$ is positive for t,u-channels and negative for s-channel. Also unparticle propagator can interfere with that of Standard Model particles like real photon and Z-boson.

3.5 Coupling to SM

In order to compute phenomenological observables, we need to describe explicitly interactions between unparticle and SM operators. In the beginning, the only constraint on SM operators is that it is expected to be invariant under Lorentz transformation. We can limit this interaction further by assuming that unparticle operators as well as SM operators are gauge invariant. All of the possible couplings of scalar unparticle operator to SM operator, under this circumstances, can be found in [33]. Scalar unparticle operators may couple to SM gauge bosons at leading order in Λ in the following way

$$\mathcal{L}_1 = \frac{\lambda_\gamma}{\Lambda_U^{d_U}} F_{\mu\nu} F^{\mu\nu} O_U$$

where λ_γ is the coupling constant and Λ_U is an energy scale which suppresses non-renormalizable couplings. Also, d_U is the scaling dimension of scalar unparticle operator O_U. In a similar way, we can show the interaction that is derived from four point coupling between scalar unparticle and fermions, again at the leading order in Λ_U. There are possible two terms [7]

$$\mathcal{L}_2 = \frac{e\lambda_f}{\Lambda_U^{d_U}} O_U \; h \; \bar{f}_L f_R \; + \; \frac{e\lambda_f^{'}}{\Lambda_U^{d_U}} \; \partial^\mu O_U \bar{f}_{L,R} \gamma_\mu f_{L,R}$$

where electromagnetic coupling e is inserted for convenience.

After the electroweak symmetry breaking, the Higgs boson will gain a vacuum expectation value $\langle h \rangle = v$: vev $\simeq 246$ Gev. Therefore first term becomes

$$\frac{e\lambda_f}{\Lambda_U^{d_U}} O_U \; v \; \bar{f}_L f_R.$$

For the second term by using integration by parts, the vector component vanishes and the axial-vector component, because of the Dirac's equation, is proportional to fermionic mass m_f. The first term is now proportional to vev and $m_f \gg v \simeq 246$ GeV (Of course top quark is excluded here). Hence the first term dominates the interaction, So, we can write

$$\mathcal{L}_2 = \frac{e\lambda_f}{\Lambda_U^{d_U}} O_U \; v \; \bar{f}_L f_R$$

By using all the information we described so far we can write the following Feynman rules for the scalar unparticle interactions with fermions and photons as as well as

gluons:

$$O_U f\bar{f} \text{ vertex } : \quad V = \frac{ie\lambda_f}{\Lambda_U^{d_U}} v P_R \tag{3.47}$$

$$O_U\gamma\gamma \ , \ O_U gg \text{ vertices : } \quad V^{\mu\nu}(p_1,p_2) = \frac{4ie\lambda_{\gamma,g}}{\Lambda_U^{d_U}}(-p_{12}g^{\mu\nu} + p_1^\nu.p_2^\mu) \tag{3.48}$$

respectively in momentum space. We set $\lambda_{\gamma,g} = 1$ and $\lambda_f = \sqrt{2\pi}/e$ for simplicity.

3.6 Virtual Unparticle Effects

The unparticle propagator has a unique structure. The phase in the propagator can lead to some interesting processes as well as interfere with Z-boson propagator. Also because of the term $\sin(d_U\pi)$ in the denominator, the propagator is singular. We now focus on processes governed by unparticle self interactions as well as some other unparticle exchanges. However, in all cases unparticles are all virtual. We will solely concern some processes such as $e^+e^- \to 4\gamma$, $e^+e^- \to 2\gamma 2\ell$, $e^+e^- \to 4g$, $e^+e^- \to 2\gamma 2g$, and $e^+e^- \to 4\ell$. Diagrams for these processes can be mediated by 3-point function of unparticle self interactions and by $s-$ and $t-$ channels with one or two unparticle exchanges.

CHAPTER 4

NUMERICAL ANALYSIS

In collider physics there are some tools which are generally called as kinematic variables, which are useful to do numerical analysis. Before proceeding the signal analysis of the processes at hand, let us briefly describe some of these kinematical variables that are going to be employed in the numerical analysis.

4.1 Some Kinematical Variables

If we consider head-on collision of two beams in the lab frame, the momentum of each particle produced in the collision can be decomposed into two components; parallel and perpendicular to beam line. If the beam line is chosen as the z-axis, the perpendicular to that direction becomes the xy plane. One of the kinematic variables that we are going to use is the transverse momentum, We may define it as

$$p_T = p \sin\theta_{CM} \tag{4.1}$$

where θ_{CM} is the scattering angle between direction of outgoing particle and collision axis. The transverse momentum p_T spans an angle φ with x-axis as shown in the left panel of 4.1. Variables involving only transverse components such as transverse momentum and azimuthal angle are invariant under longitudinal boosts. Therefore it would be better write the phase space element in terms of these variables in cylindrical coordinates [34],

$$\frac{d^3p}{E} = dp_x dp_y \frac{dp_z}{E} = p_T dp_T d\varphi \frac{dp_z}{E} \ . \tag{4.2}$$

It can be easily demonstrated that $\dfrac{dp_z}{E}$ is also Lorentz invariant under the longitudinal boosts.

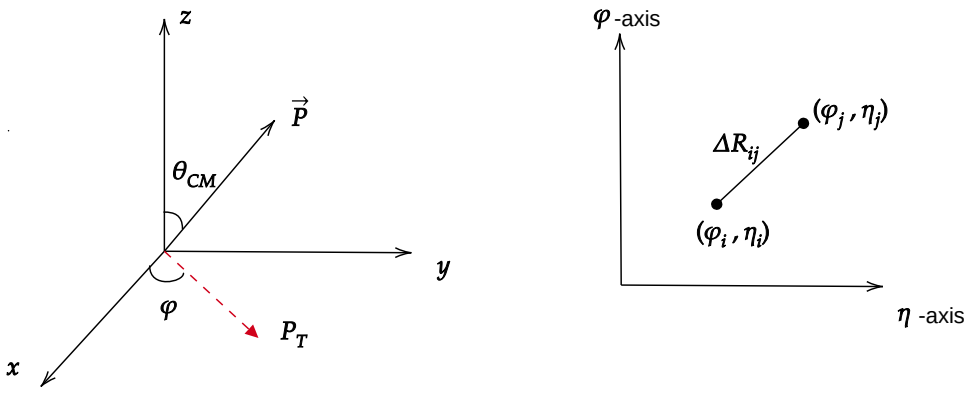

Figure 4.1: Definition of transverse momentum and definition of particle distance (cone size) in the $\phi - \eta$ plane

Another variable which is used for the numerical analysis is the so-called pseudo-rapidity. It is generically used to measure the scattering angle. As pseudo-rapidity is a special form of rapidity, let us first try to understand what rapidity is. It is generally defined as

$$y = \frac{1}{2} \ln \left(\frac{E + p_z}{E - p_z} \right) . \tag{4.3}$$

In a boosted frame, $E \to \gamma(E - \beta p_z),\ p_z \to \gamma(p_z - \beta E)$, the rapidity becomes

$$y' = \frac{1}{2} \ln \left(\frac{(1-\beta)(E+p_z)}{(1+\beta)(E-p_z)} \right) = y + \ln \left(\frac{1-\beta}{1+\beta} \right) = y - y_0 . \tag{4.4}$$

Hence, even if rapidity is not invariant under longitudinal boosts, the difference between two rapidities is invariant.

In the massless case , $E^2 = |\vec{p}|^2 + m^2 \to E = |\vec{p}|^2$, the rapidity can be written as

$$y \to \frac{1}{2} \ln \left(\frac{1 + \cos\theta_{CM}}{1 - \cos\theta_{CM}} \right) = -\ln \left(\tan \frac{\theta_{CM}}{2} \right) \equiv \eta . \tag{4.5}$$

This is named as pseudo-rapidity. It is more useful than rapidity to do analysis as the mass of particles in a collider are generically neglected, because center of mass energy is much higher compared to mass of particles. The phase space can also be rewritten as

$$\frac{d^3p}{E} = p_T dp_T d\varphi d\eta . \tag{4.6}$$

Another kinematical variable which is invariant under longitudinal boosts is the cone size or separation between the i^{th} and j^{th} particles in the $\eta - \varphi$ plane as shown in the

right panel of 4.1. It can be defined as

$$\Delta R_{ij} = \sqrt{(\varphi_i - \varphi_j)^2 + (\eta_i - \eta_j)^2} \tag{4.7}$$

where φ_i is the azimuthal angle and η_i is pseudo-rapidity of particle i.

Having introduced some of the relevant kinematical variables, it would be timely to mention briefly physics of CLIC experiment.

4.2 Physics of CLIC

Electron-positron colliders may provide some advantages compared to hadron colliders. First, e^-e^+ interaction is mostly understood within the electroweak theory and we can make predictions on SM processes with great success. Second, a system involving e^- and e^+ has zero charge and zero lepton number. Therefore it is suitable to create new particles. Another advantage is that it is possible to have high degrees of polarization. Furthermore since electron and positron are elementary particles, it is a clean environment which can allow precise studies of SM particles especially Higgs particle and the top quark. Moreover, it can lead to direct search opportunities for BSM theories in a new experimental environment. So, in a sense, an e^-e^+ collider may be complementary to hadron colliders.

The Compact Linear Collider (CLIC) is the first multi-TeV high luminosity linear e^-e^+ collider expected to be built at CERN after LHC will shut down. CLIC is expected to be operated in three different center of mass energies at different stages.

The first stage will operate at the center of mass energy 380 GeV to study Higgs physics and top quark with a precision that cannot be reached by even high luminosity LHC. Higher energy stages is expected to be at 1.5 TeV and 3 TeV. These energies may enhance precision test of SM. Also they can provide direct or indirect searches for BSM theories. CLIC is assumed to provide $\pm 80\%$ longitudinal polarisation for electron beams. At the beginning stage no positron polarisation is planned. However, CLIC is also compatible with introducing positron polarisation. Therefore, in addition to $\pm 80\%$ longitudinal polarisation for the electron beam, $\pm 30\%$ longitudinal polarisation for the positron beam is also assumed in this thesis.

For the signals that we will concentrate on, the following basic selection cuts for each process is presented in Table 4.1. Total cross sections computed for each channel is listed in Table 4.2 at center of mass energy $\sqrt{s} = 3$ Tev for $d_U = 1.1,\ 1.5,\ 1.9$ with $\Lambda_U = 1$ Tev. The SM cross-sections are listed for background-signal comparison.

Table 4.1: The selection cuts imposed for each channel

$e^-e^+ \to 4\gamma$	$e^-e^+ \to 2g2\gamma$	$e^-e^+ \to 2\gamma2\ell$	$e^-e^+ \to 4\ell$	$e^-e^+ \to 4g$
$p_T(\gamma) > 50$ GeV	$p_T(\gamma) > 50$ GeV	$p_T(\gamma) > 50$ GeV	$p_T(\ell) > 100$ GeV	$p_T(g) > 50$ GeV
	$p_T(g) > 50$ GeV	$p_T(\ell) > 100$ GeV		
$\lvert\eta(\gamma)\rvert < 4$	$\lvert\eta(\gamma)\rvert < 4$	$\lvert\eta(\gamma)\rvert < 4$	$\lvert\eta(\ell)\rvert < 2.5$	$\lvert\eta(g)\rvert < 4$
	$\lvert\eta(g)\rvert < 4$	$\lvert\eta(\ell)\rvert < 2.5$		
	$\Delta R(g,g) > 0.8$	$\Delta R(\ell,\ell) > 0.6$		
$\Delta R(\gamma,\gamma) > 0.6$	$\Delta R(\gamma,\gamma) > 0.6$	$\Delta R(\gamma,\gamma) > 0.6$	$\Delta R(\ell,\ell) > 0.6$	$\Delta R(g,g) > 0.8$
	$\Delta R(\gamma,g) > 0.6$	$\Delta R(\gamma,\ell) > 0.6$		

Table 4.2: The total cross-sections in pb of the signals for $\Lambda_U = 1\text{TeV}$ at various values of d_U.

Cross-section values (pb)					
Process	Λ_U	$d_U = 1.1$	$d_U = 1.5$	$d_U = 1.9$	SM
$e^-e^+ \to 4\gamma$	1 TeV	0.00987	0.00248	0.00288	0.00146
$e^-e^+ \to 4e$	1 TeV	0.00190	0.00107	0.00106	0.00103
$e^-e^+ \to 4\mu$	1 TeV	0.000068	0.000027	0.000032	0.000021
$e^-e^+ \to 4g$	1 TeV	9.98	3.20	7.90	–
$e^-e^+ \to 2e2\gamma$	1 TeV	0.037	0.024	0.025	0.021
$e^-e^+ \to 2e2\mu$	1 TeV	0.0021	0.00112	0.001116	0.001073
$e^-e^+ \to 2\gamma2\mu$	1 TeV	0.0033	0.0011	0.0014	0.00078
$e^-e^+ \to 2g2\gamma$	1 TeV	0.063	0.0060	0.0080	–

4.3 The process $e^+e^- \to 4\gamma$

To carry out the simulations of the processes chosen, as mentioned above, there are various kinematical variables one can use to cast better the new physics scenario

in comparison with the standart model predictions. Among them, we choose three of them, namely cone size ΔR_{ij} between final state particle sets, psuedo-rapidity η_i of particles, and the transverse momenta p_T of final state particles. Throughout the numerical analysis, the followings will be kept the same, namely the center of mass energy of CLIC, $\sqrt{s} = 3$ TeV, the integrated luminosity of the collider, $\mathcal{L} = 2000\,\mathrm{fb}^{-1}$, and the polarization of the electrons and positrons ($P_{e^-} = 80\%$ and $P_{e^+} = 30\%$).

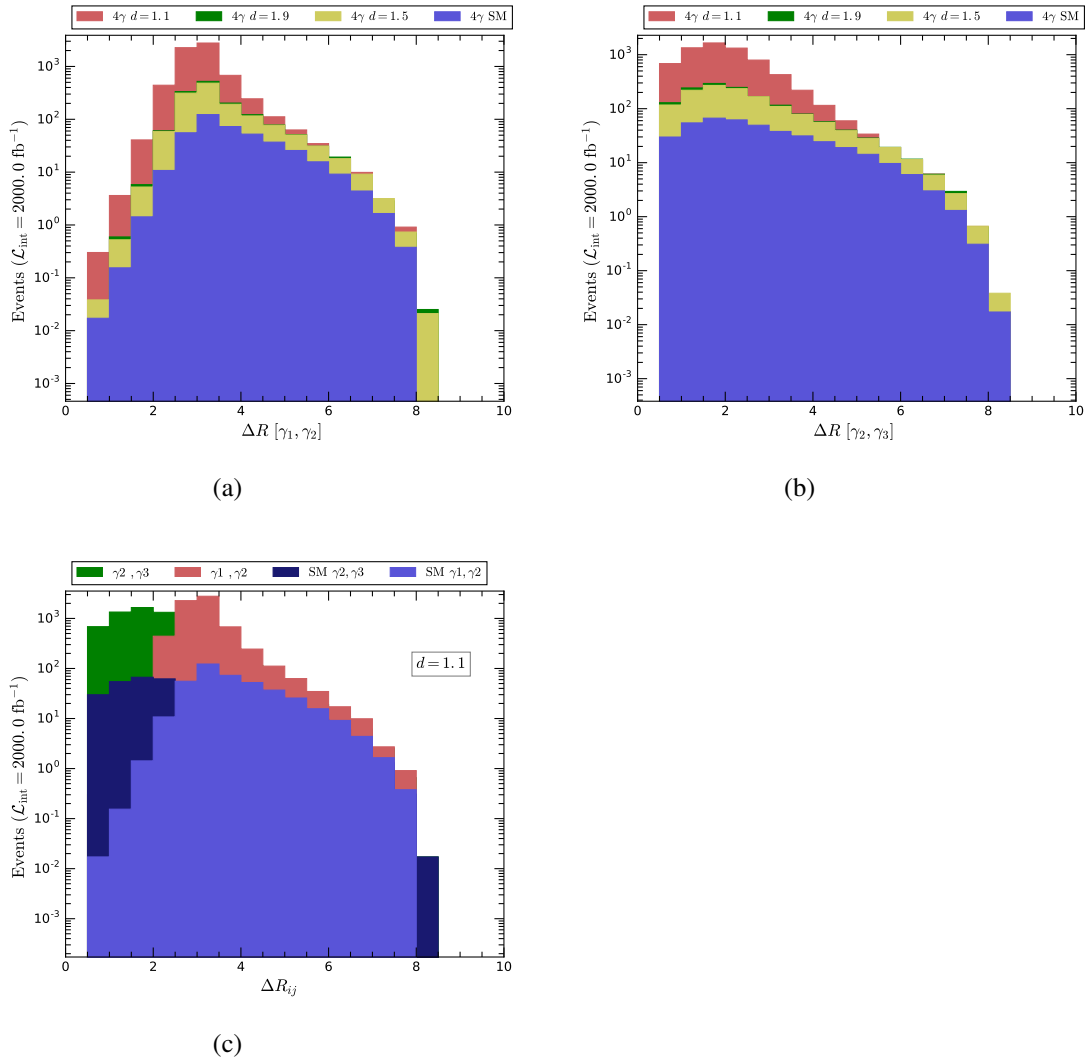

(a) (b)

(c)

Figure 4.2: Various distributions of the process $e^+e^- \to 4\gamma$ in the framework of unparticle stuff with $\sqrt{s} = 3\,\mathrm{TeV}$ at CLIC

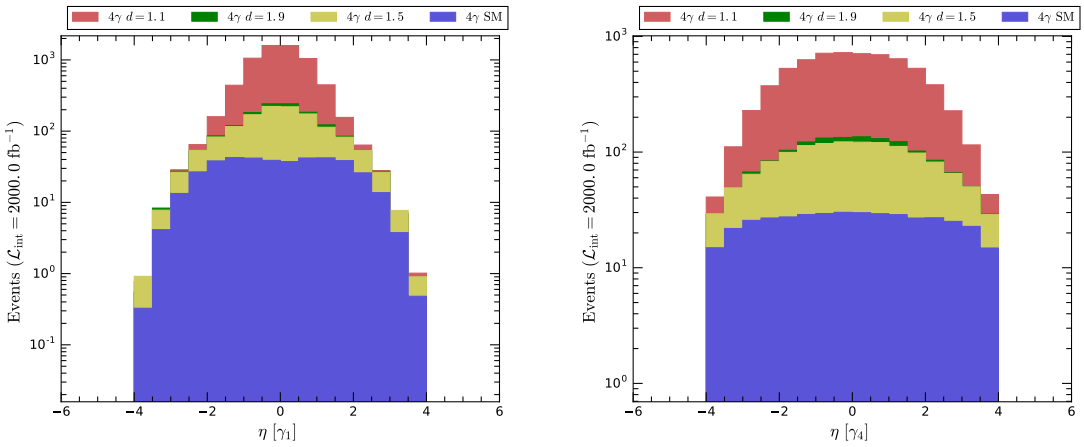

(a) (b)

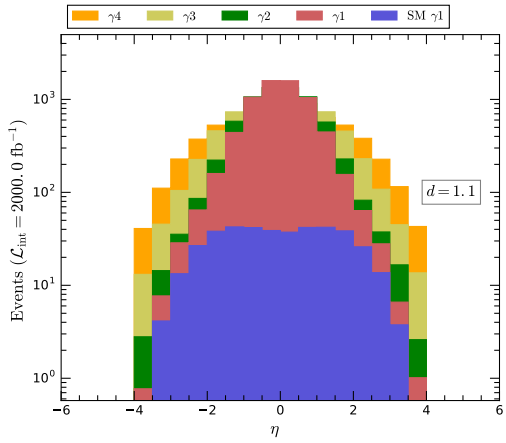

(c)

Figure 4.3: Various distributions of the process $e^+e^- \to 4\gamma$ in the framework of unparticle stuff with $\sqrt{s} = 3\,\mathrm{TeV}$ at CLIC

In Figures (4.2) to (4.4), number of events of the process $e^+e^- \to 4\gamma$ is depicted as a function of the kinematical variables $\Delta R_{ij}, \eta_i$, and P_{Ti} in various combinations for both the SM and the unparticle scenario. As far as ΔR_{ij} distributions are concerned, they are given in Figures (4.2a), (4.2b), and (4.2c). In Figure (4.2a), number of events are shown as a function of the cone size between the hardest and the second hardest photons (ΔR_{12}) for various values scaling dimension d. The SM background is also included. A similar distribution for ΔR_{23} is displayed in Figure (4.2b). In both cases, the SM shows similar pattern with much less number of events and as the scaling dimension d gets larger, the unparticle scenario approaches to the SM case

and indeed after $d = 1.5$, the sensivity to d disappears. Moreover the peak value shift to smaller ΔR values as one considers ΔR_{23} instead of ΔR_{12}. It means that in most of the events expected the hardest photon and the second hardest one are very well separated as compared to the second and third hardest ones. Indeed if one considers the second and fourth or the third and fourth the separation would become smaller and smaller and most of the events are not going to be useful since the minimum cut on ΔR_{ij}, which is taken to be 0.4 and then 0.6, would make them difficult to be identified properly. This shows why it is rather hard to isolate four photons separately as a signal. In Figure (4.2c), number of events is shown as a function of ΔR_{12} and ΔR_{23} for the best unparticle scenario (that is, the $d = 1.1$ case).

In Figure (4.3), the pseudo-rapidity histograms are given. We prefer to display the distributions only for the hardest photon (η_1) in Fig. (4.3a) as well as the softest photon (η_4) in Fig. (4.3b). The third graph (Fig. (4.3b)) shows all four photon's psuedo-rapidities for $d = 1.1$ case. Due to the cut $|\eta_i| < 4$ for all photons, no distribution is shown outside that region. First of all, all the distributions are symmetric with respect to $\eta = 0$. If we concentrate on the hardest photon, it has a sharp peak at $\eta = 0$, which is the transverse plane, for $d = 1.1$ and even though the peak position does not shift for larger d values, it gets broader. In the SM case it is much more flattened. The situation for the least energetic photon shows more wider distribution as given in Fig. (4.3b). Fig. (4.3c) shows how the η distributions of all photons gets wider as compared to the hardest photon of the SM, which is way smaller and wider than the unparticle case. In this sense, restricting η in a narrower region would help to eliminate most of the background events.

The last set of graphs for the process $e^+e^- \to 4\gamma$ are given in Figs. (4.4) which are about p_T distributions of photons. In Fig. (4.4a), the hardest photon peaks at large p_T while the SM one fades there. Thus, discriminating the signal photon, even for larger d values, from the background photon is rather easier and still possible for the second hardest photon as well (given inf Fig. (4.4b)). However, for the other two photons whose distributions are given in Figs. (4.4c) and (4.4d) they become more like the background and identification would be harder and require more delicate techniques. This makes the four isolated photon signal as a difficult one to observe and measure.

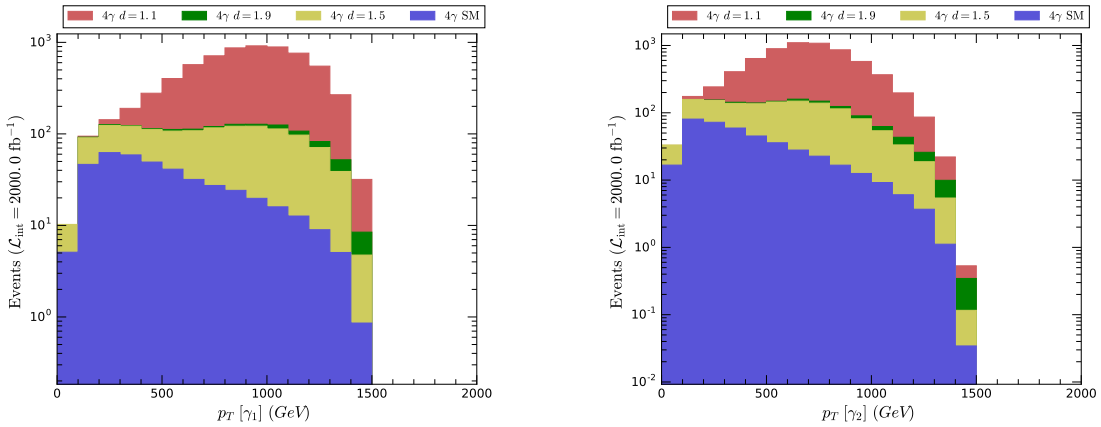

(a) (b)

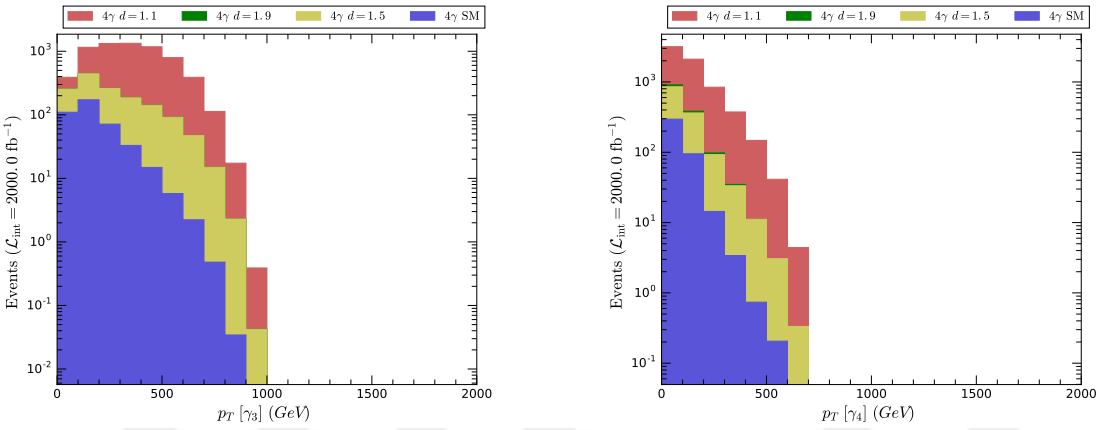

(c) (d)

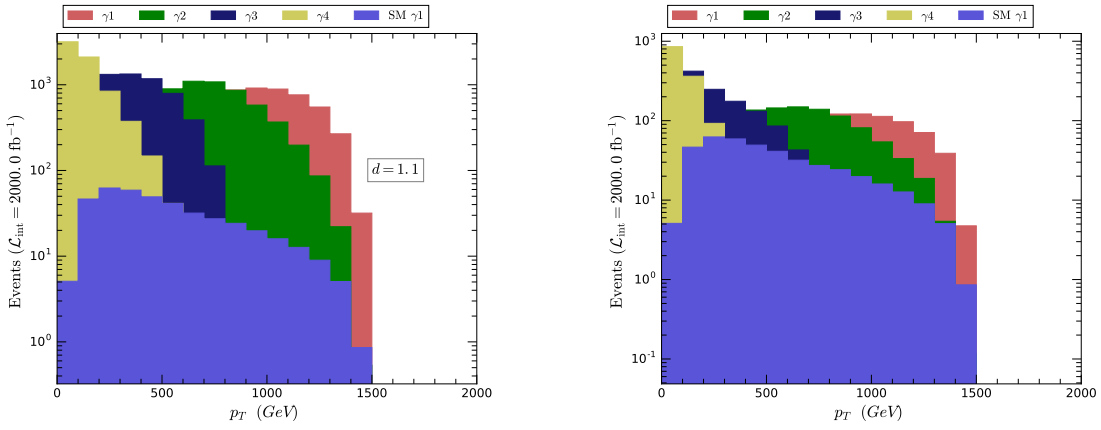

(e) (f)

Figure 4.4: Various distributions of the process $e^+e^- \to 4\gamma$ in the framework of unparticle stuff with $\sqrt{s} = 3\,\mathrm{TeV}$ at CLIC

4.4 The process $e^+e^- \to 4g$

In this section, we require four isolated gluons. The difference between this process and the process in the previous section is that it is background free. Indeed, there are contributions at one-loop level given in Figure 4.5. This is beyond the scope of the thesis.

In Figures (4.6) to (4.7) the number of events in this process is plotted as a function of various variables. Cone size has very similar patterns for different scaling dimension. Also pseudo-rapidity histograms seem to not distinguish from each other as scaling dimension changes. Nothing much can be said unless a background study has been carried out.

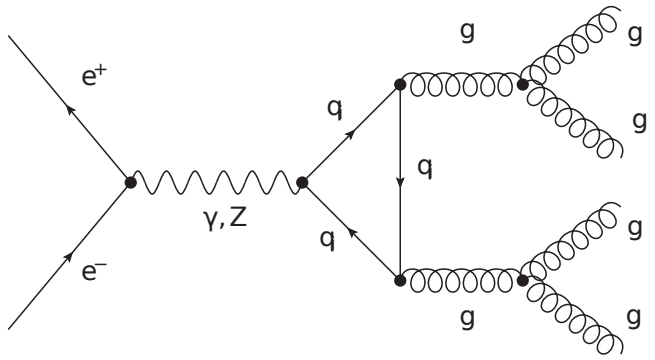

Figure 4.5: A sample diagram contributing $e^+e^- \to 4g$ at one-loop in the SM.

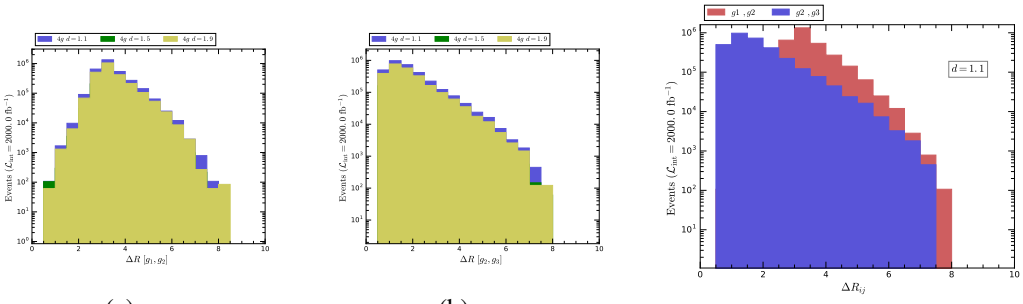

(a) (b) (c)

Figure 4.6: Various distributions of the process $e^+e^- \to 4g$ in the framework of unparticle stuff with $\sqrt{s} = 3\,\mathrm{TeV}$ at CLIC

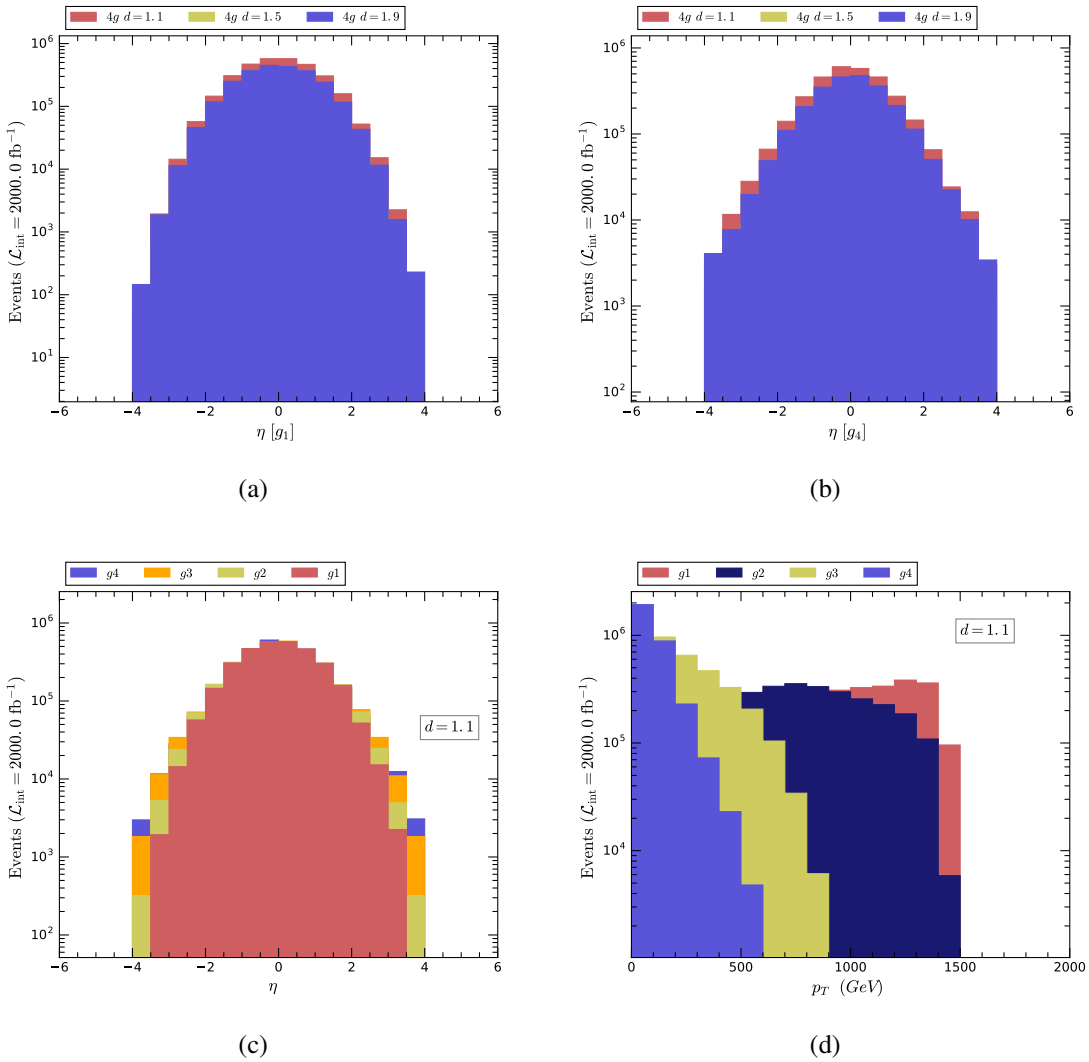

(a) (b)

(c) (d)

Figure 4.7: Various distributions of the process $e^+e^- \to 4g$ in the framework of unparticle stuff with $\sqrt{s} = 3\,\mathrm{TeV}$ at CLIC

4.5 The process $e^+e^- \to 2\gamma 2g$

This process is very similar to $e^+e^- \to 4g$ and again there is no background at three level. The distributions are given in Figures 4.8, 4.9, and 4.10. Without doing a background analysis at one-loop, further discussion of the signal wouldn't be not suitable.

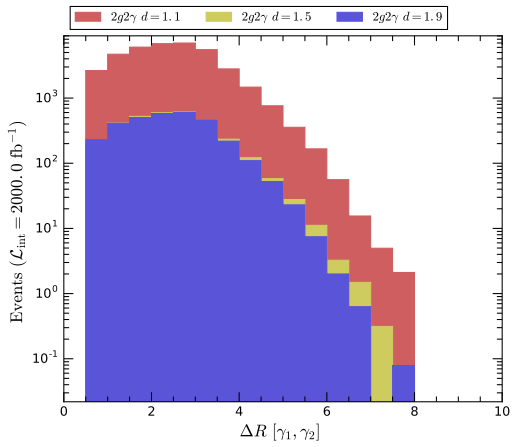

(a)

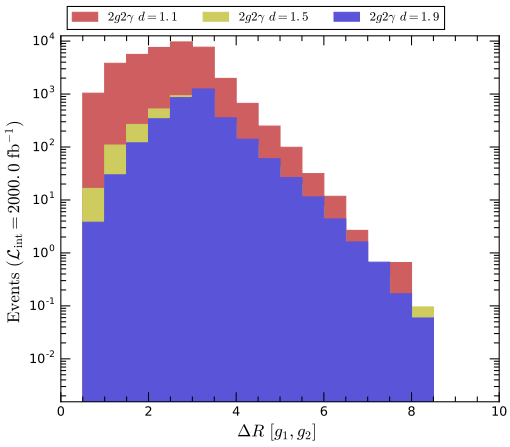

(b)

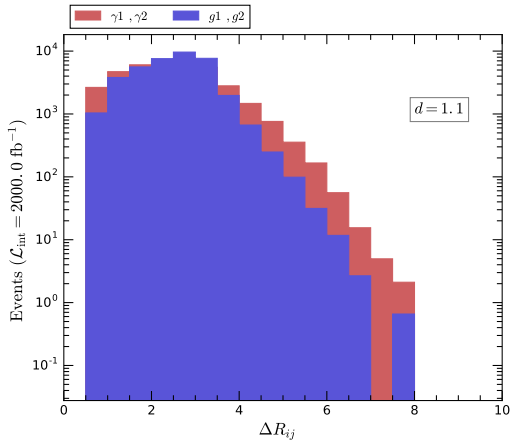

(c)

Figure 4.8: Various distributions of the process $e^+e^- \to 2\gamma 2g$ in the framework of unparticle stuff with $\sqrt{s} = 3\,\mathrm{TeV}$ at CLIC

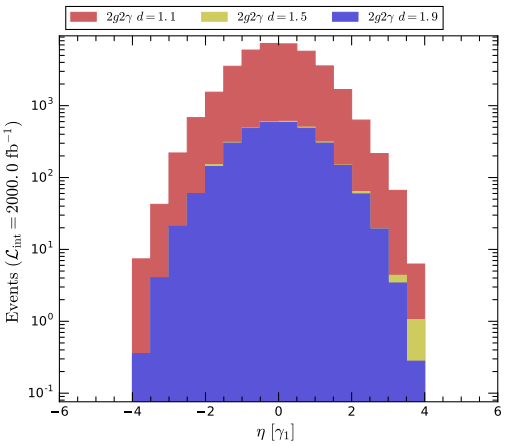

(a)

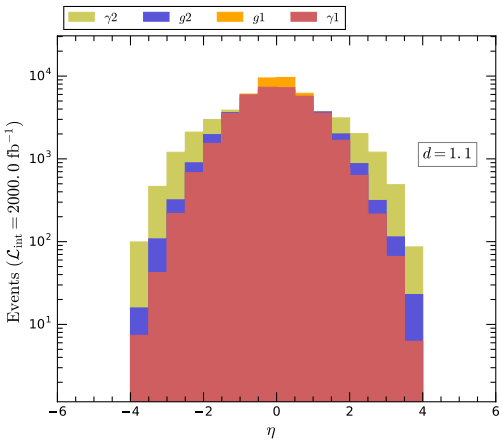

(b)

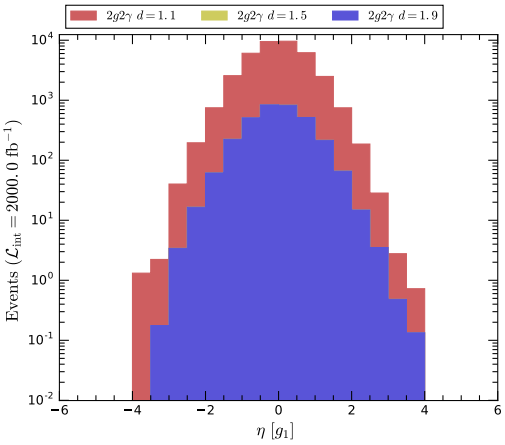

(c)

Figure 4.9: Various distributions of the process $e^+e^- \to 2\gamma 2g$ in the framework of unparticle stuff with $\sqrt{s} = 3\,\mathrm{TeV}$ at CLIC

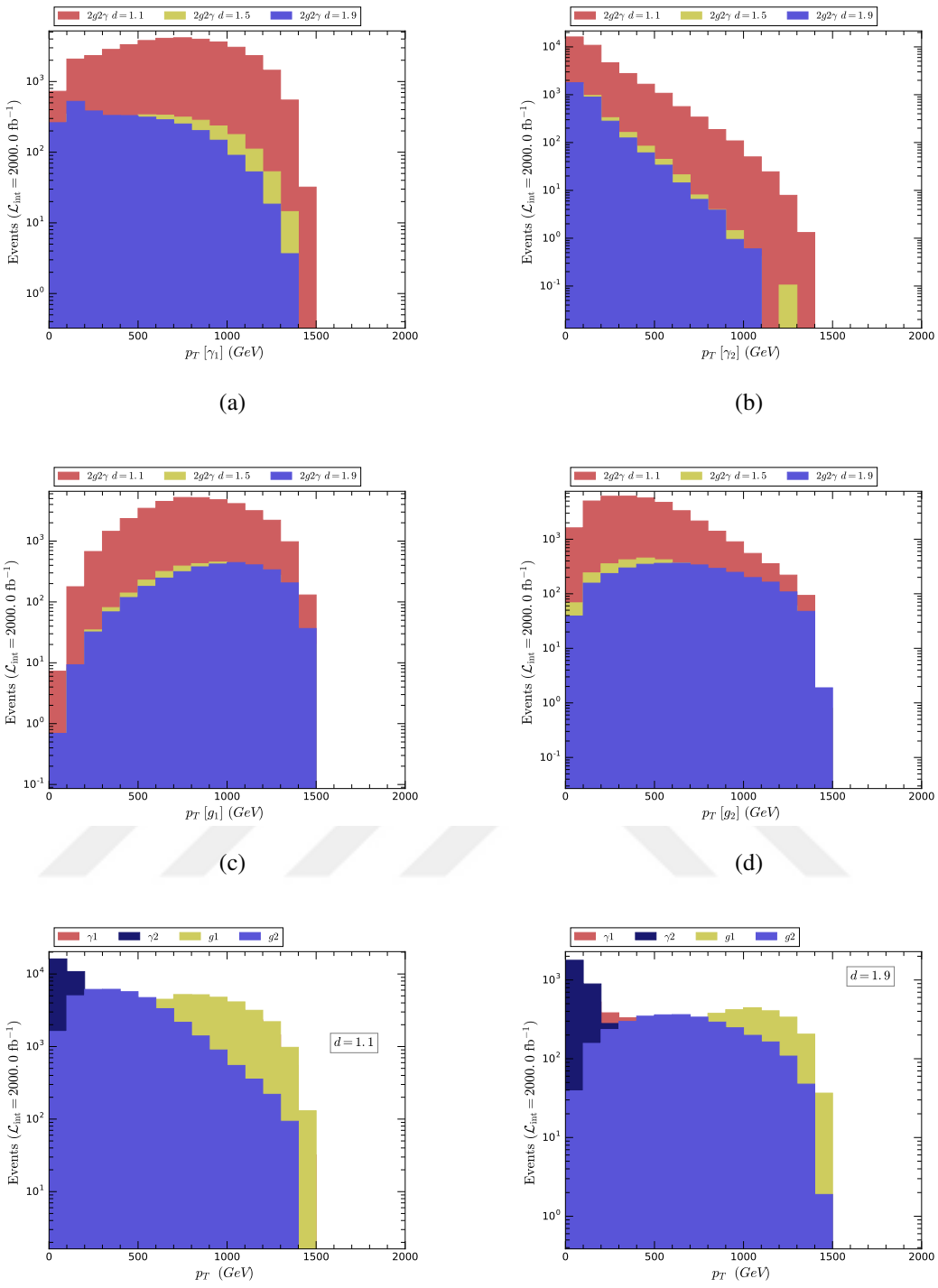

Figure 4.10: Various distributions of the process $e^+e^- \to 2\gamma 2g$ in the framework of unparticle stuff with $\sqrt{s} = 3\,\mathrm{TeV}$ at CLIC

4.6 The process $e^+e^- \to 2e2\gamma$

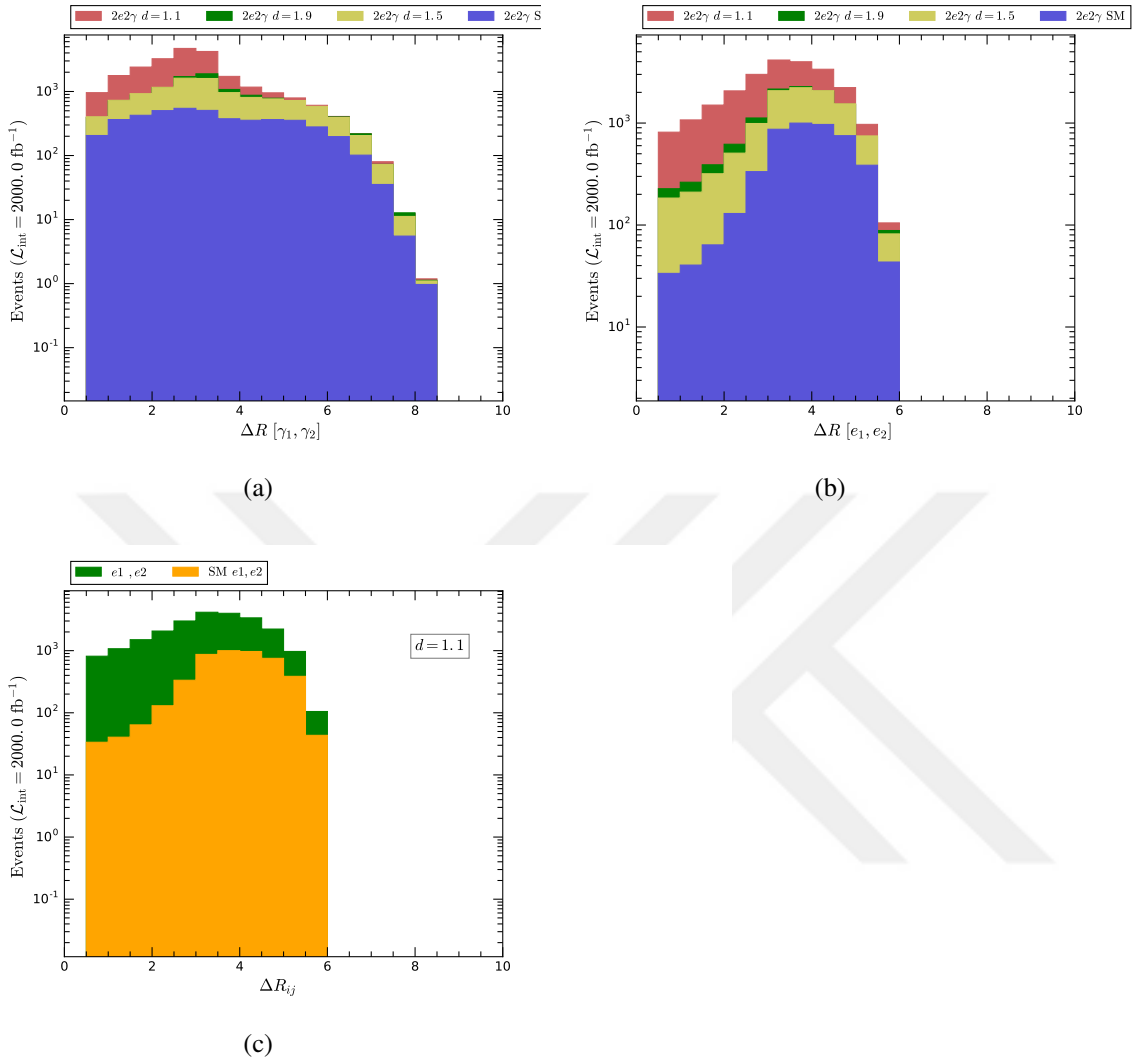

(a) (b)

(c)

Figure 4.11: Various distributions of the process $e^+e^- \to 2e2\gamma$ in the framework of unparticle stuff with $\sqrt{s} = 3\,\mathrm{TeV}$ at CLIC

In this section, we need two isolated photons and two isolated electrons in the final state. The results are demonstrated in Figures (4.11) to (4.13). In Figures (4.11a), (4.11b), the distributions with respect to the cone size between photon pairs and electron pairs are depicted. As in the case of $e^-e^+ \to 4\gamma$. the SM has similar features as like the unparticle case. In Figure (4.12), the pseudo-rapidity graphs are shown. We take only the hardest photon and the hardest electron into consideration. While the unparticle case has a sharp peak around $\eta[\gamma_1] = 0$, especially for $d = 1.1$, we observe that the

peak position shifts for the SM and because of that it can be an useful variable to discriminate the signal from the background. The number of events as a function of transverse momenta of photons is also presented in (4.13).

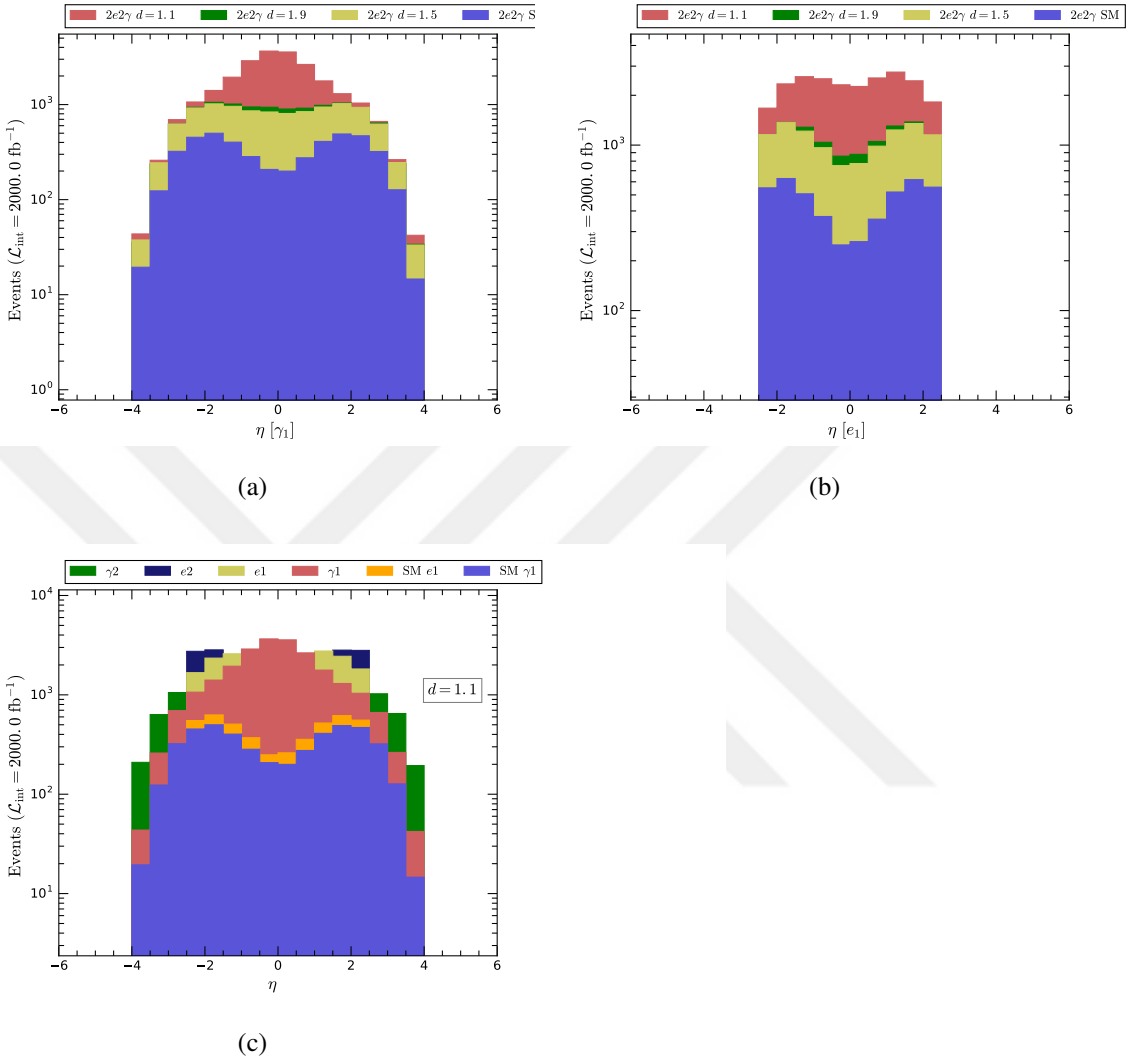

Figure 4.12: Various distributions of the process $e^+e^- \to 2e2\gamma$ in the framework of unparticle stuff with $\sqrt{s} = 3\,\mathrm{TeV}$ at CLIC

4.7 The process $e^+e^- \to 2\mu 2\gamma$

In this section, we consider the signal with two isolated photons and two isolated muons. Our findings are shown in figures 4.14 to 4.16.

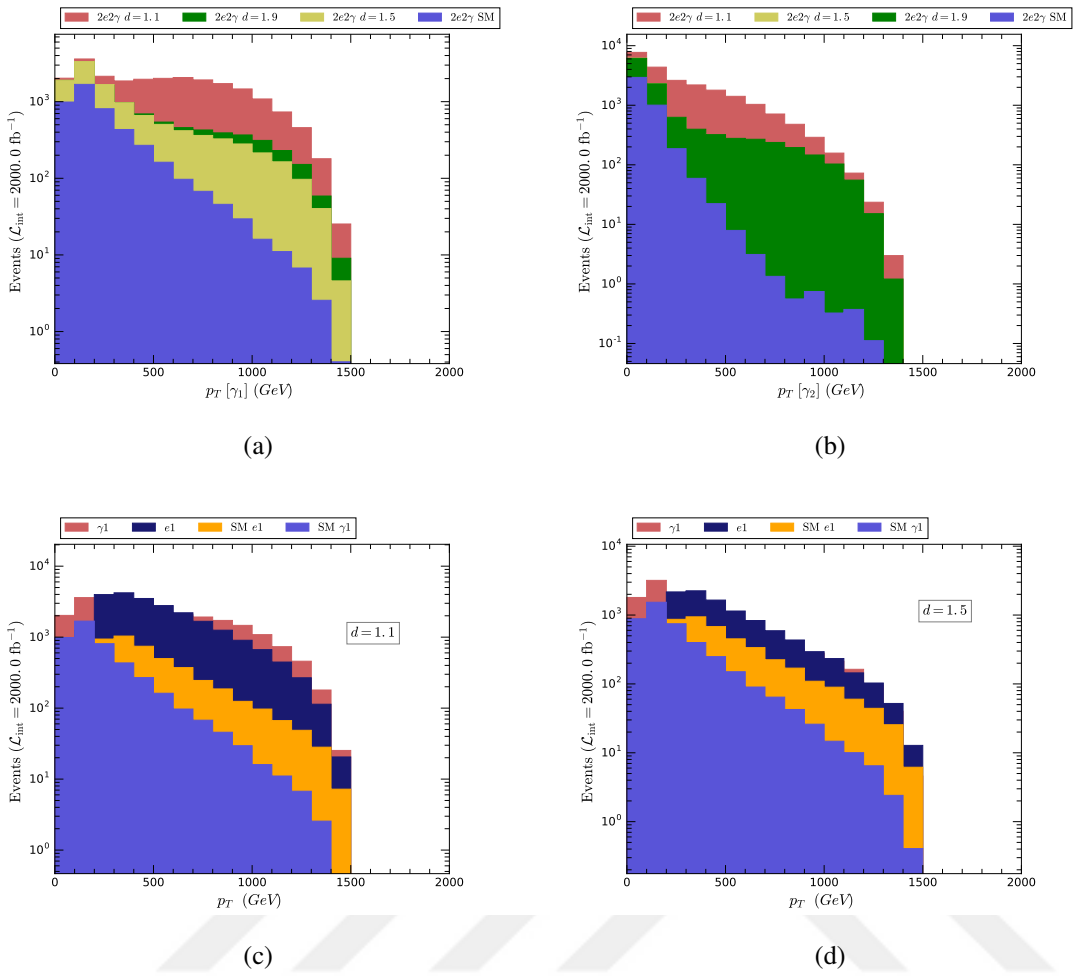

Figure 4.13: Various distributions of the process $e^+e^- \to 2e2\gamma$ in the framework of unparticle stuff with $\sqrt{s} = 3\,\mathrm{TeV}$ at CLIC

For example, in figure 4.15a, the hardest photon seems to have a peak at $\eta = 0$ for $d = 1.1$ and for larger d values, it gets broader. The background is more flattened. In figure 4.15b, the hardest muon shows a narrower distribution compared to the hardest photon.

In figure 4.16, p_T histograms for the hardest and the second hardest photon and muon are depicted. It seems possible to discern the signal from background for hardest and even for second hardest photon. However, as far as muons are concerned, signal does not show profound differences from background.

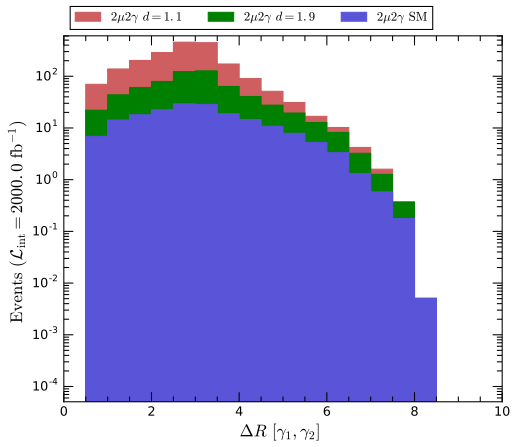

(a)

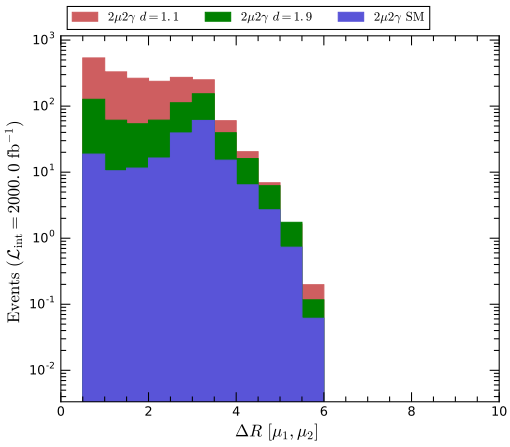

(b)

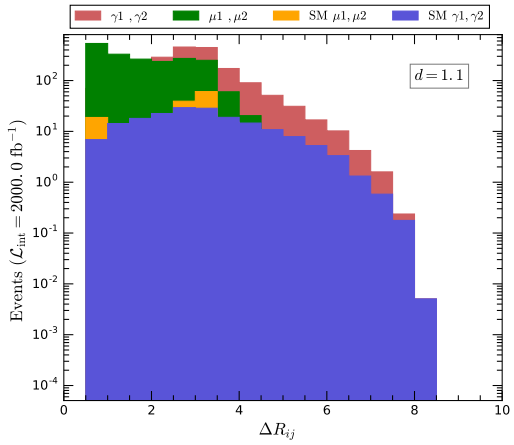

(c)

Figure 4.14: Various distributions of the process $e^+e^- \to 2\mu2\gamma$ in the framework of unparticle stuff with $\sqrt{s} = 3\,\mathrm{TeV}$ at CLIC

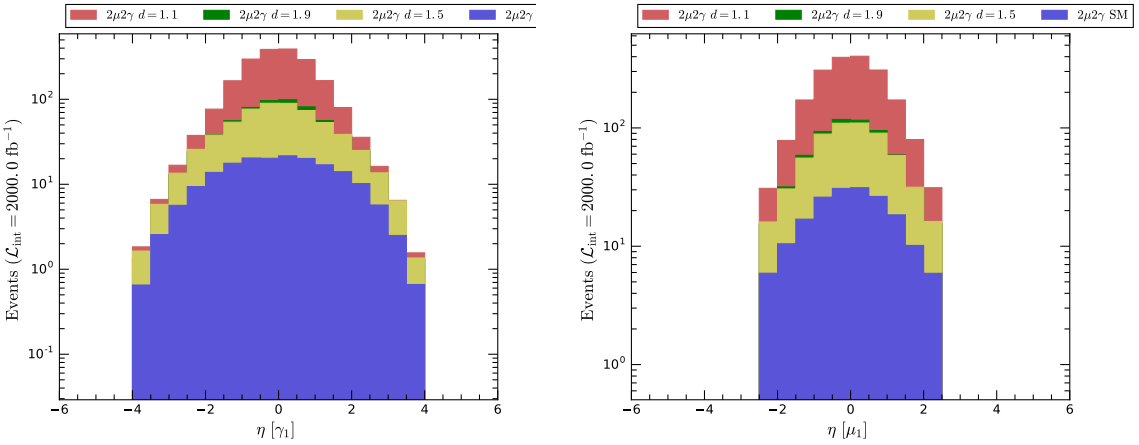

(a)

(b)

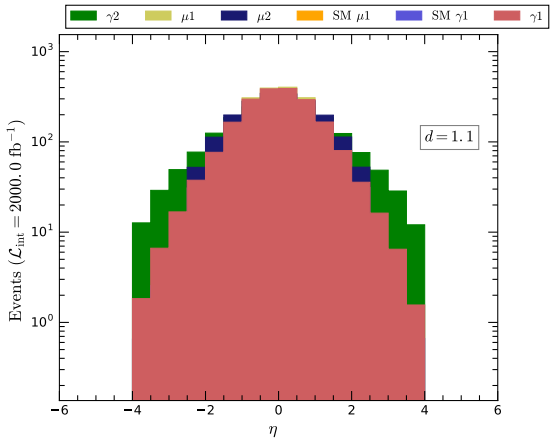

(c)

Figure 4.15: Various distributions of the process $e^+e^- \to 2\mu2\gamma$ in the framework of unparticle stuff with $\sqrt{s} = 3\,\mathrm{TeV}$ at CLIC

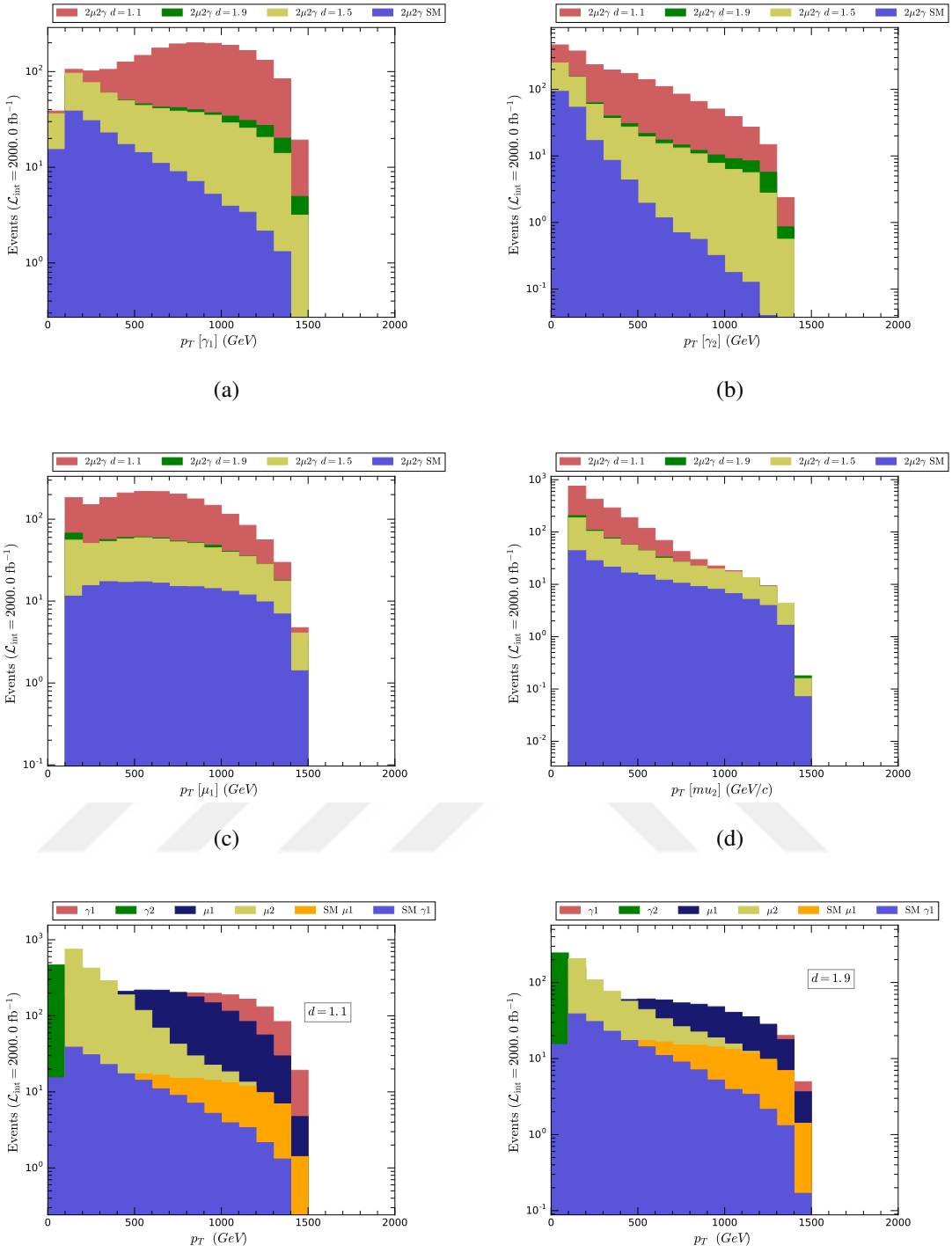

Figure 4.16: Various distributions of the process $e^+e^- \to 2\mu2\gamma$ in the framework of unparticle stuff with $\sqrt{s} = 3\,\mathrm{TeV}$ at CLIC

4.8 The process $e^+e^- \to 4\ell$

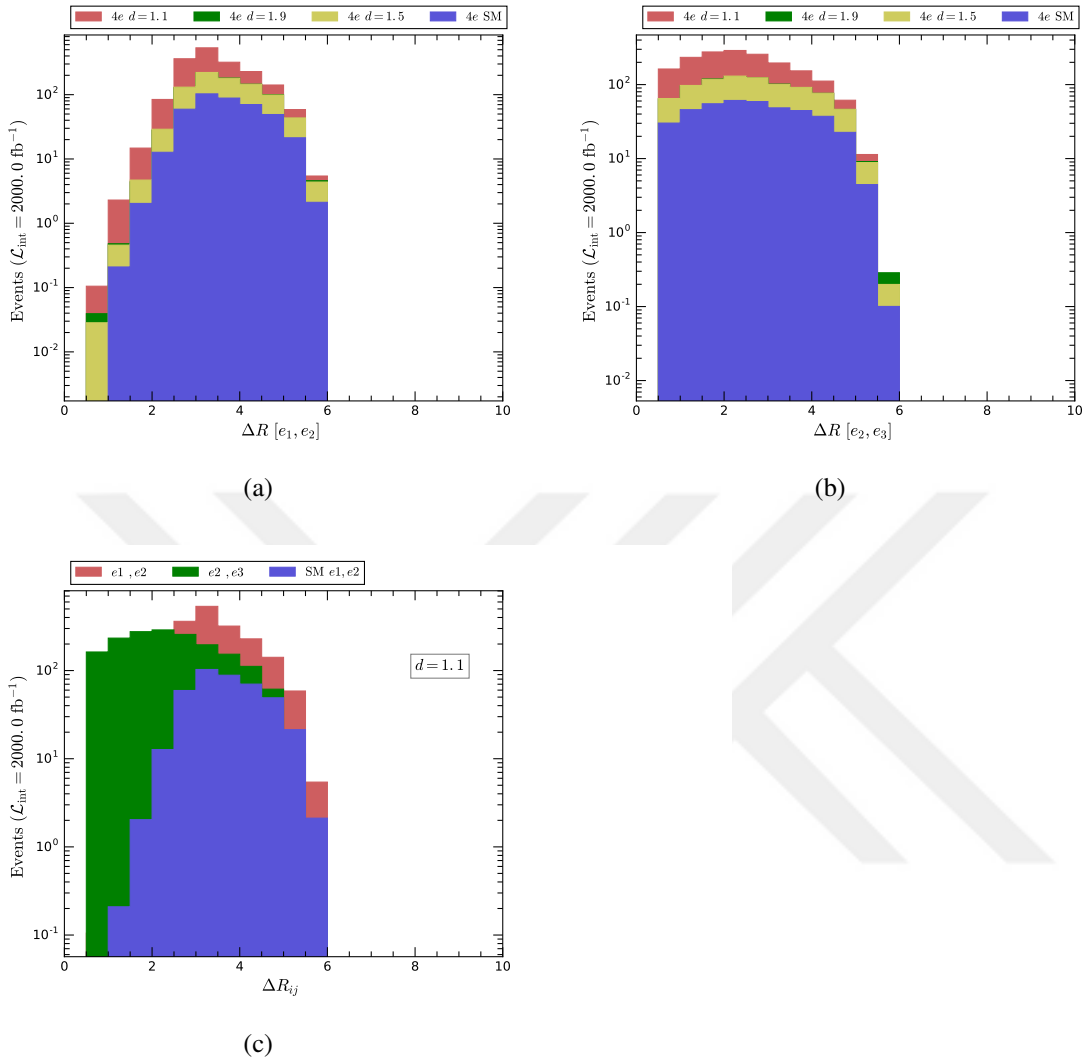

(a) (b)

(c)

Figure 4.17: Various distributions of the process $e^+e^- \to 4e$ in the framework of unparticle stuff with $\sqrt{s} = 3\,\mathrm{TeV}$ at CLIC

In this section, we study signal with four isolated leptons which can be either solely electrons ($4e$) or solely muons (4μ) or electron and muon pairs ($2e2\mu$). Particularly, in this section we investigate possible differences in distributions regarding the fermion flavor. The results are presented in Figures 4.17 to 4.19, 4.20 to 4.22 and 4.23 to 4.25. As far as separation between the hardest and the second hardest lepton is considered, signal and background resemble each other for all processes. However more events are produced in the case of $4e$ compared to other 4ℓ signals. This is somehow

expected result since the number of Feynman diagrams in $4e$ signal (655 diagrams) are much more than that of the 4μ signal (220 diagrams) and the $2e2\mu$ signal (239 diagrams). Related to this, it seems to have larger cross-section.

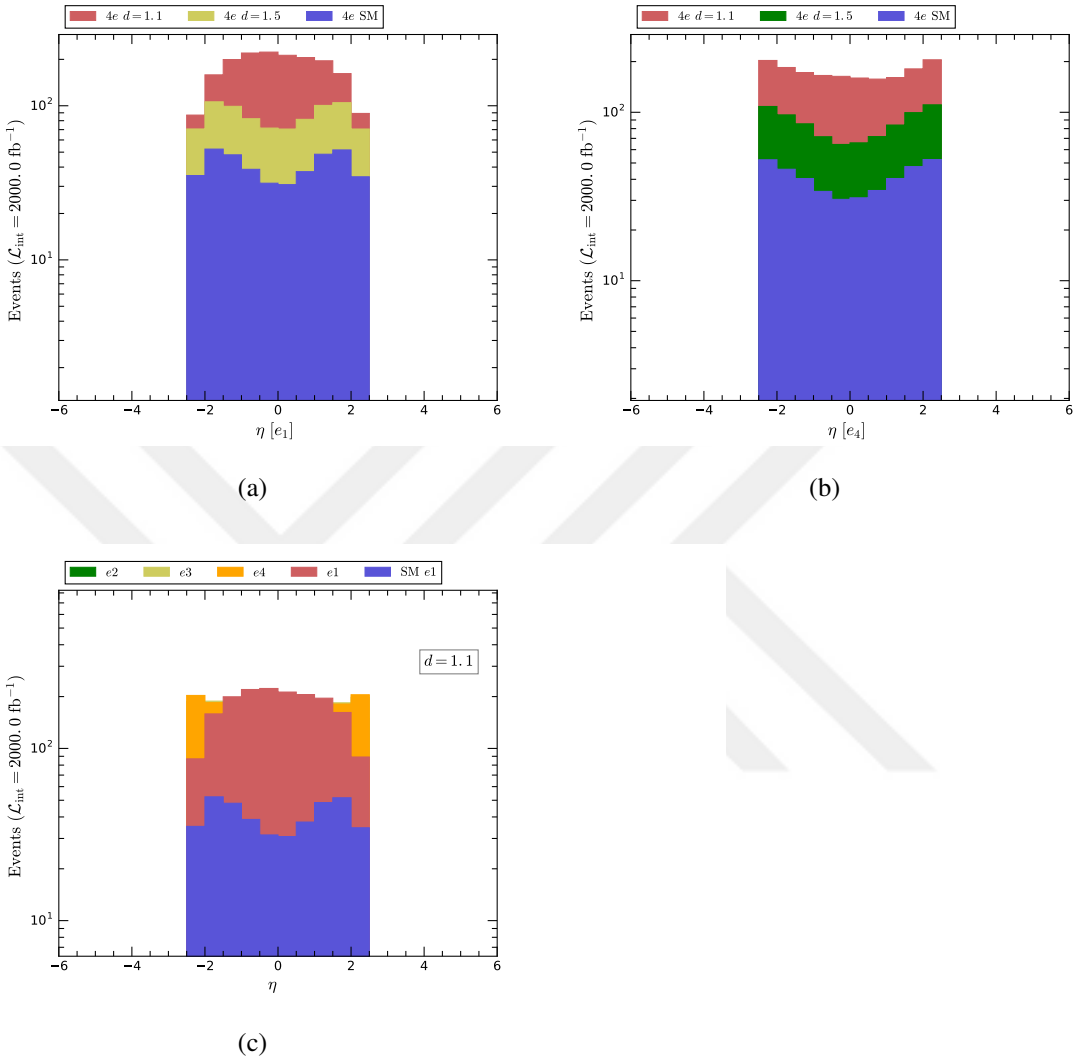

Figure 4.18: Various distributions of the process $e^+e^- \to 4e$ in the framework of unparticle stuff with $\sqrt{s} = 3\,\mathrm{TeV}$ at CLIC

Pseudo-rapidity distributions are shown in figures 4.18 , 4.21 , 4.24. Let us focus on the most energetic electron for the $e - e+ \to 4e$ process. While the SM has a sharp peak around $|\eta| = 2$ which corresponds to $\theta_{CM} \simeq 15°$, the unparticle distribution is more flattened for $d = 1.1$. As the scaling dimension gets larger values, the SM and unparticle cases start to resemble each other. In the $2e2\mu$ process, the hardest muon

seems to have a sharper peak at $\eta = 0$ for $d = 1.1$. Distributions for larger d values approach to the SM distributions.

The summary of the results are all listed in Table 4.3. For each signal, total cross section, number of signal events as well as the $S/(S+B)$ ratio are presented for three values of the scaling dimension $d_U = 1.1, 1.5, 1.9$. As seen the best $S/(S+B)$ ratio, which is around 0.94 for $d = 1.1$, is for the signal $e^+e^- \to 4\gamma$. There are few other signals with a similar ratio but their statistics are rather lower.

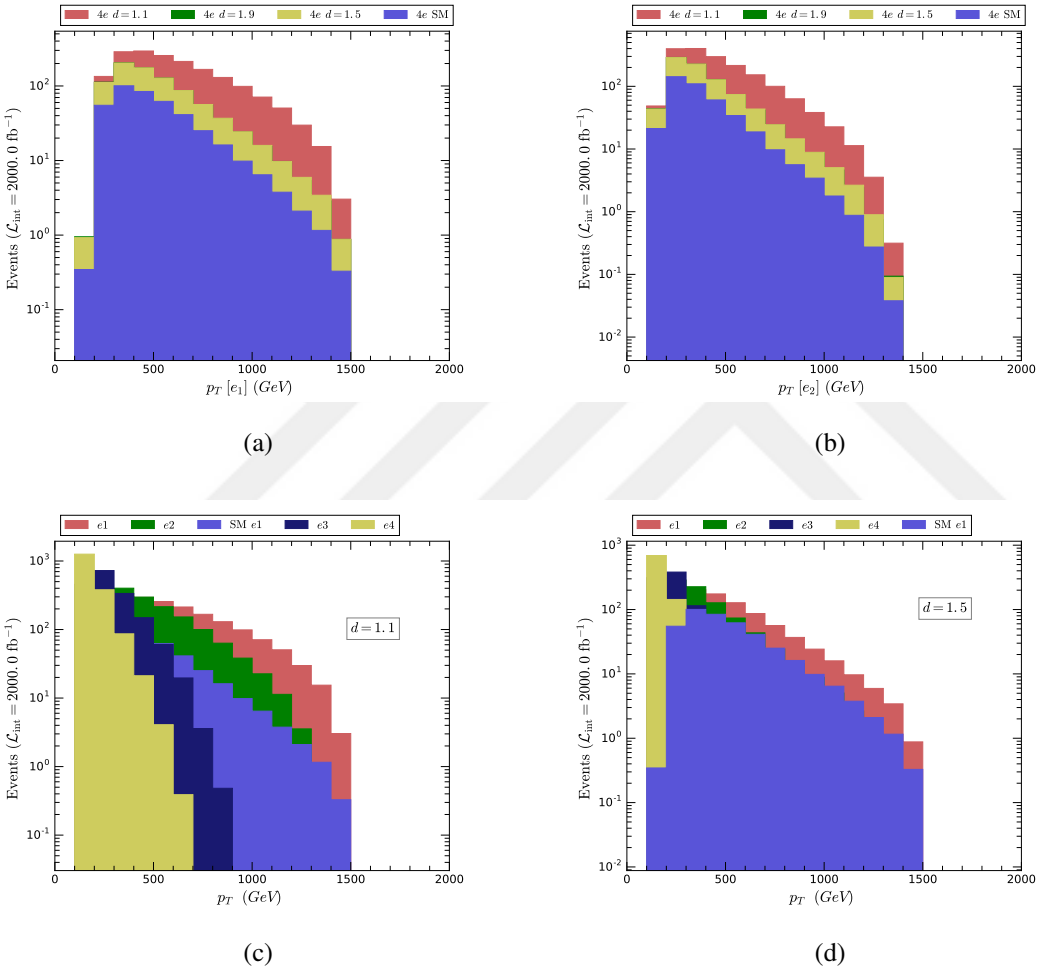

(a) (b)

(c) (d)

Figure 4.19: Various distributions of the process $e^+e^- \to 4e$ in the framework of unparticle stuff with $\sqrt{s} = 3\,\mathrm{TeV}$ at CLIC

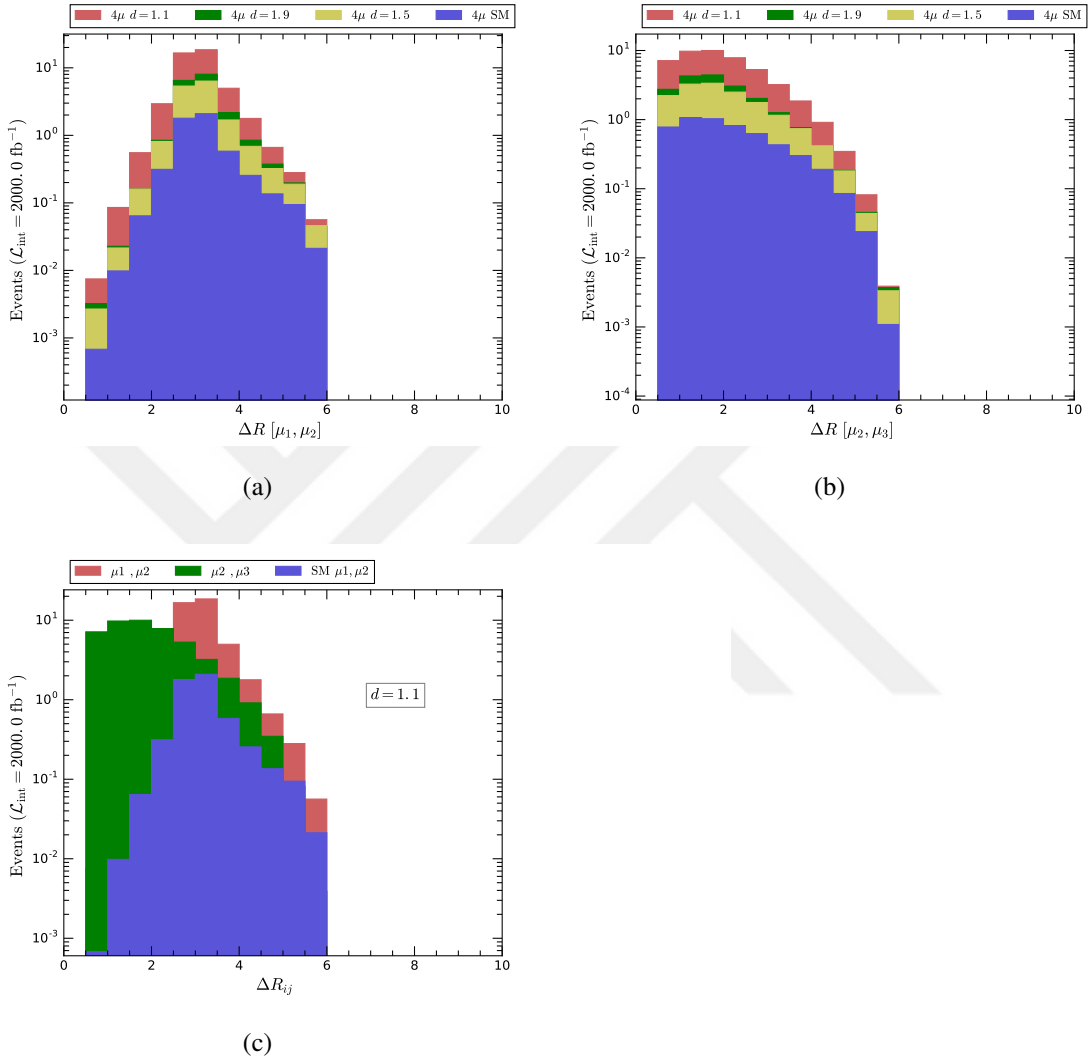

(a) (b)

(c)

Figure 4.20: Various distributions of the process $e^+e^- \to 4\mu$ in the framework of unparticle stuff with $\sqrt{s} = 3\,\mathrm{TeV}$ at CLIC

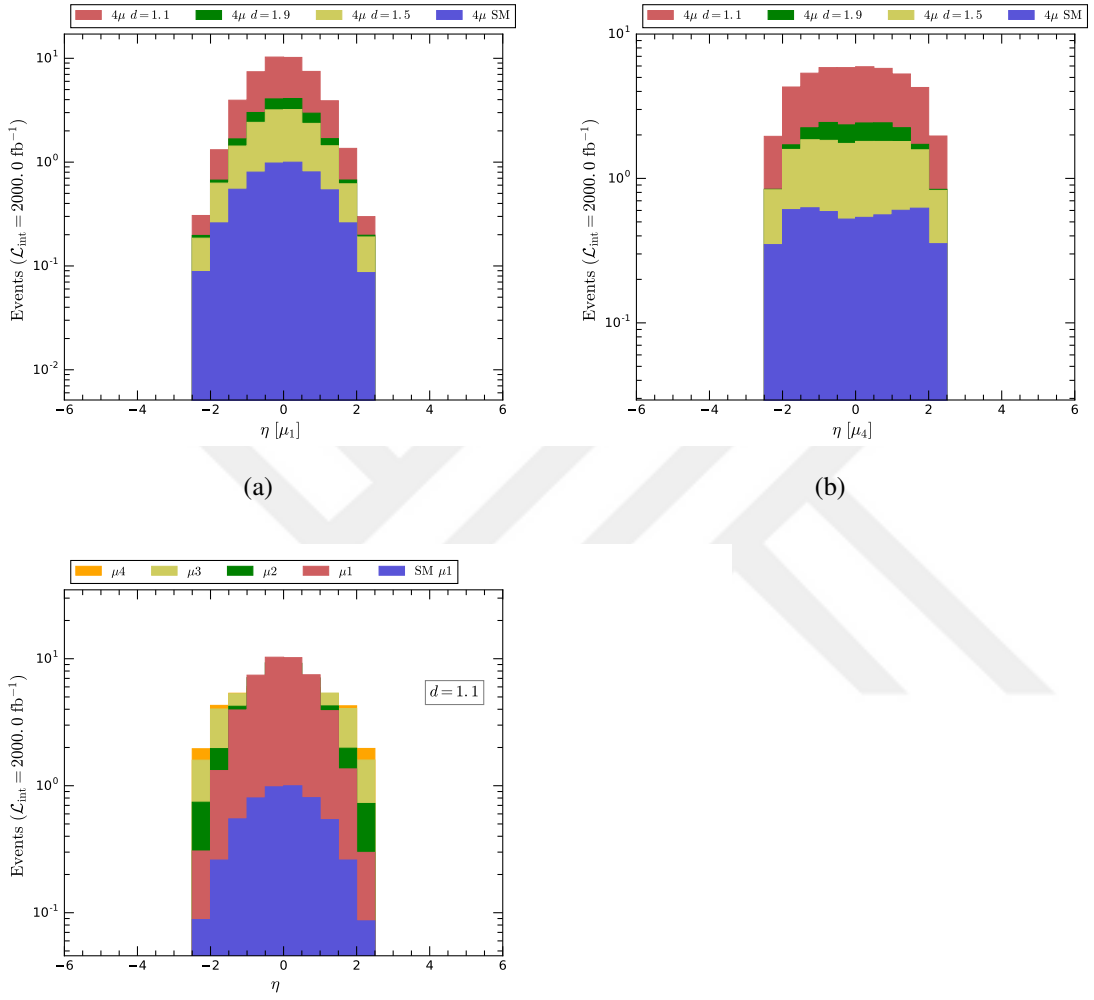

(a) (b)

(c)

Figure 4.21: Various distributions of the process $e^+e^- \to 4\mu$ in the framework of unparticle stuff with $\sqrt{s} = 3\,\mathrm{TeV}$ at CLIC

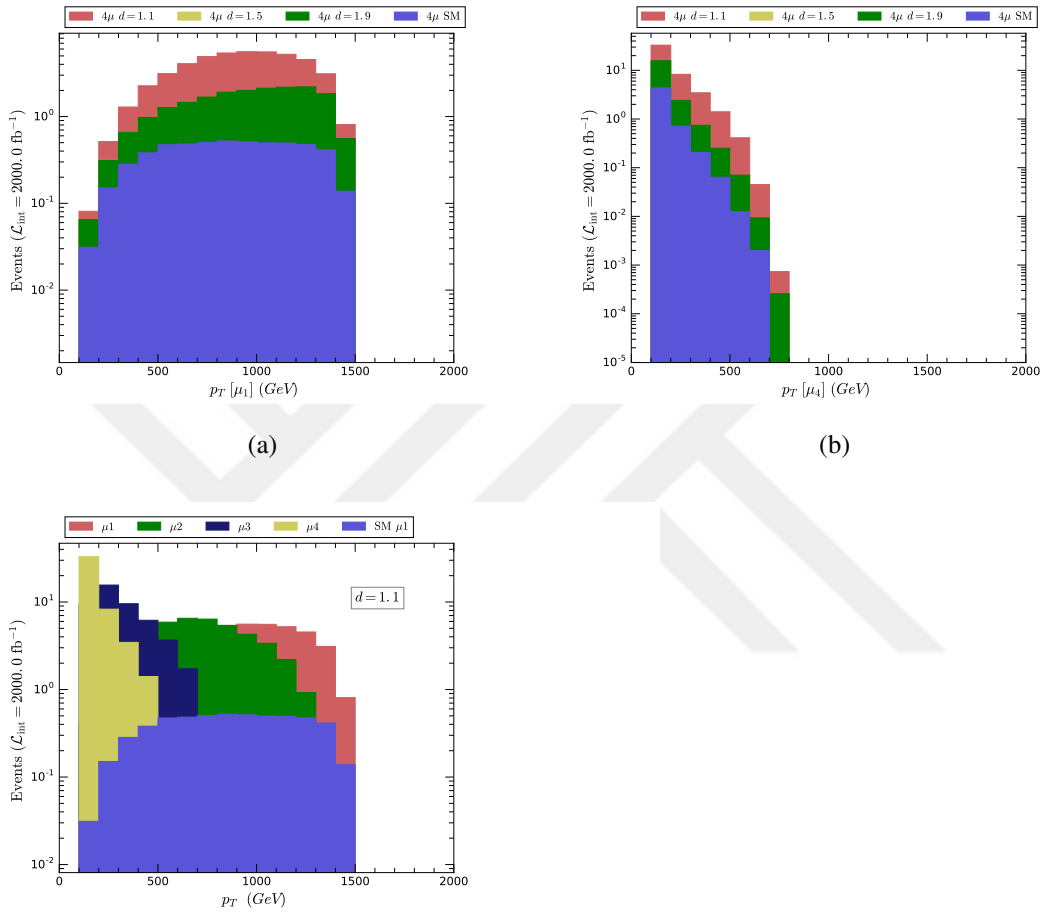

Figure 4.22: Various distributions of the process $e^+e^- \to 4\mu$ in the framework of unparticle stuff with $\sqrt{s} = 3\,\mathrm{TeV}$ at CLIC

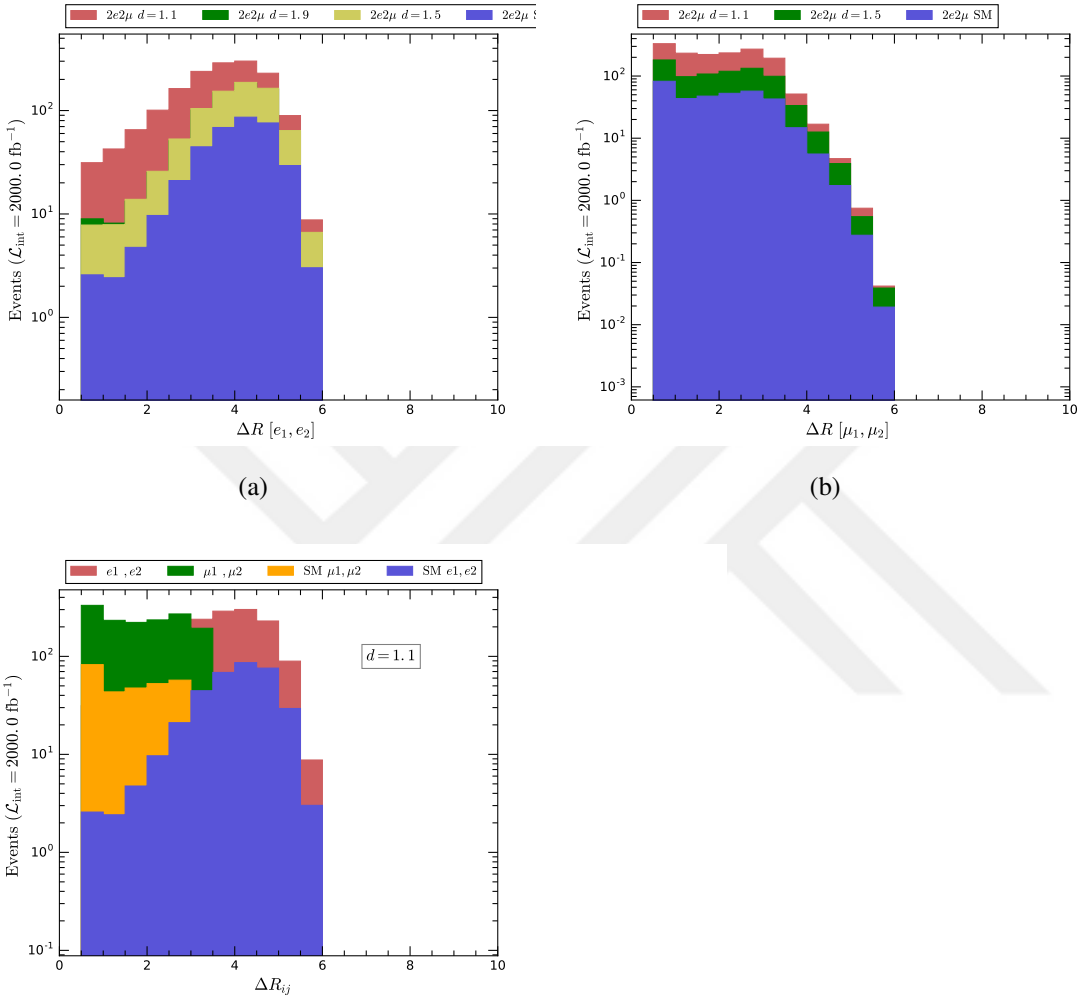

(a) (b)

(c)

Figure 4.23: Various distributions of the process $e^+e^- \to 2e2\mu$ in the framework of unparticle stuff with $\sqrt{s} = 3\,\mathrm{TeV}$ at CLIC

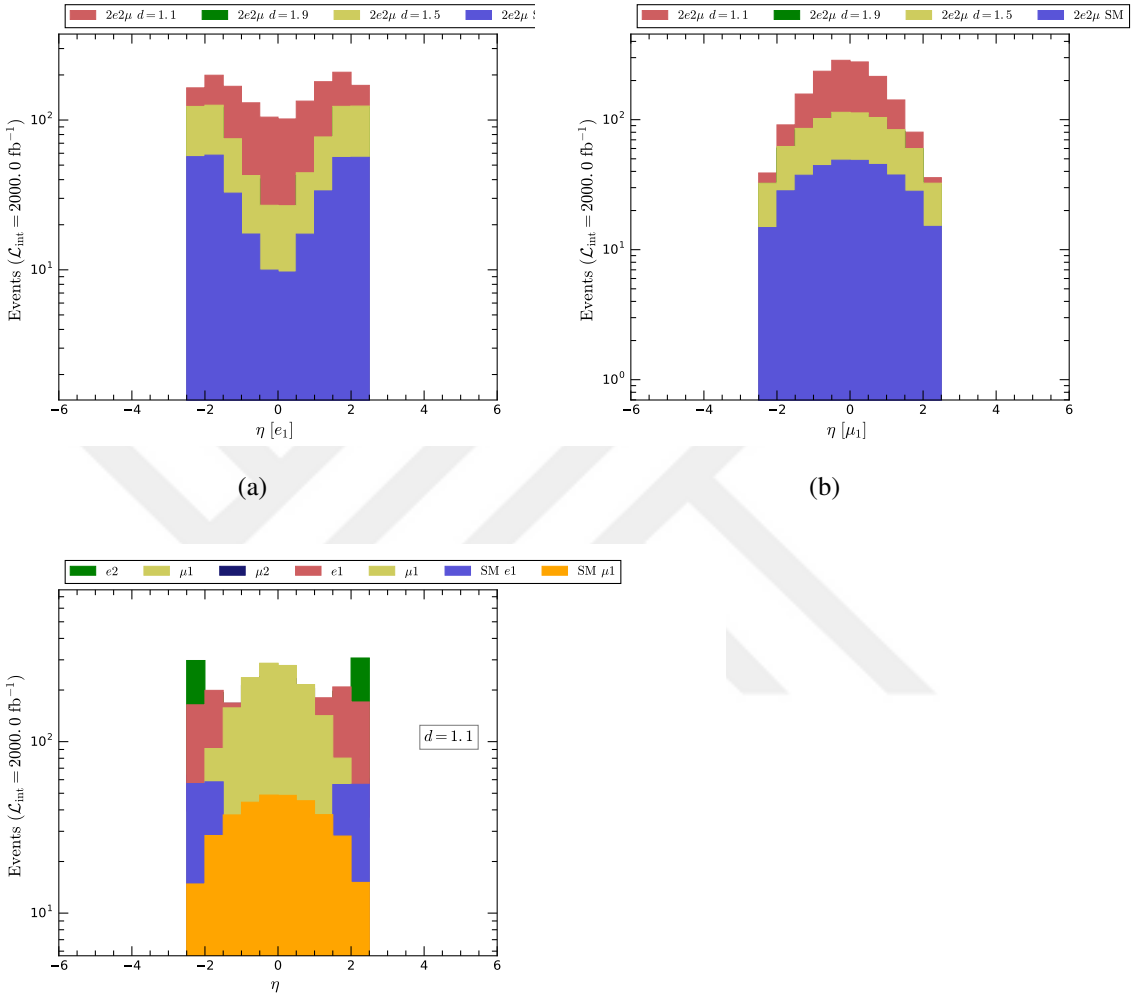

Figure 4.24: Various distributions of the process $e^+e^- \to 2e2\mu$ in the framework of unparticle stuff with $\sqrt{s} = 3\,\text{TeV}$ at CLIC

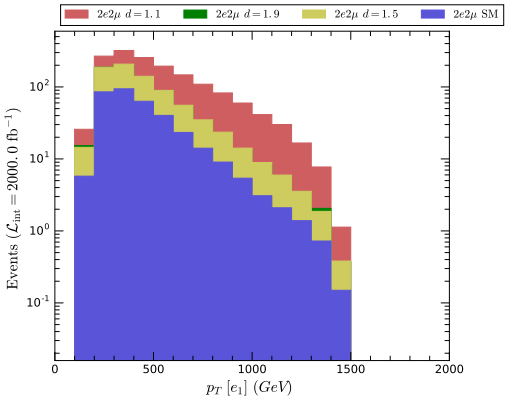

(a)

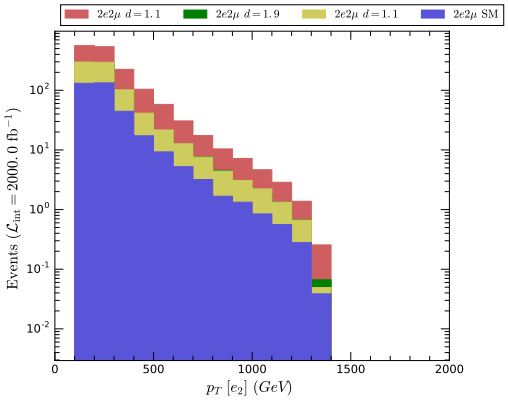

(b)

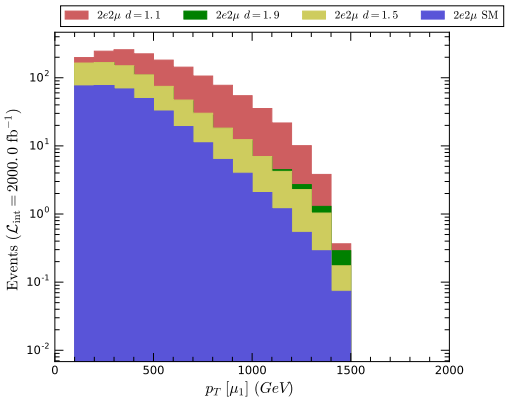

(c)

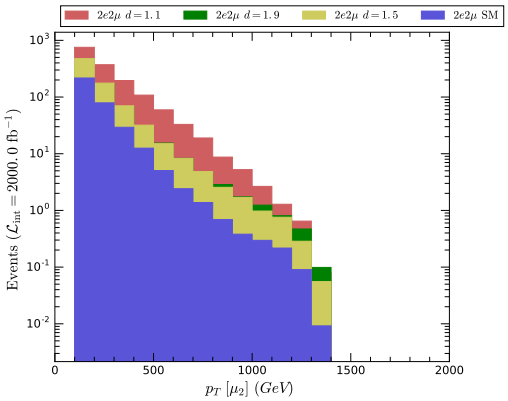

(d)

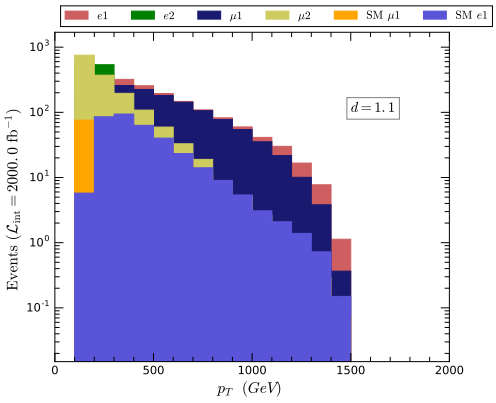

(e)

Figure 4.25: Various distributions of the process $e^+e^- \to 2e2\mu$ in the framework of unparticle stuff with $\sqrt{s} = 3\,\mathrm{TeV}$ at CLIC

Table 4.3: The summary of the numerical analysis.

Process	d_U	σ (pb)	S	$\frac{S}{S+B}$
	1.1	0.00987	6382.8 ± 66.0	0.94 ± 0.02
$e^-e^+ \to 4\gamma$	1.5	0.00248	1002.6 ± 28.3	0.71 ± 0.07
	1.9	0.00288	1102.8 ± 29.9	0.729 ± 0.063
	1.1	0.00190	1306.4 ± 29.4	0.76 ± 0.05
$e^-e^+ \to 4e$	1.5	0.00107	449.8 ± 18.9	0.522 ± 0.104
	1.9	0.00106	439.6 ± 18.7	0.516 ± 0.106
	1.1	0.000068	43.39 ± 5.43	0.885 ± 0.286
$e^-e^+ \to 4\mu$	1.5	0.000027	10.60 ± 2.92	0.652 ± 0.063
	1.9	0.000032	14.56 ± 3.36	0.721 ± 0.548
	1.1	0.037	18098 ± 118	0.804 ± 0.019
$e^-e^+ \to 2e2\gamma$	1.5	0.024	6345.5 ± 74.5	0.59 ± 0.03
	1.9	0.025	6836.2 ± 77.2	0.608 ± 0.028
	1.1	0.0033	1674.5 ± 35.3	0.867 ± 0.048
$e^-e^+ \to 2\mu2\gamma$	1.5	0.0011	424.6 ± 18.6	0.624 ± 0.106
	1.9	0.0014	502.1 ± 20.2	0.662 ± 0.096
	1.1	0.0021	1241.0 ± 29.5	0.78 ± 0.06
$e^-e^+ \to 2e2\mu$	1.5	0.0011	391.7 ± 18.0	0.528 ± 0.107
	1.9	0.0011	379.2 ± 17.7	0.52 ± 0.118
	1.1	0.06	39598 ± 168	~ 1
$e^-e^+ \to 2\gamma2g$	1.5	0.006	3324.2 ± 50.2	~ 1
	1.9	0.008	3413.5 ± 52.6	~ 1
	1.1	9.98	3147998 ± 3428	~ 1
$e^-e^+ \to 4g$	1.5	3.20	1003689 ± 1256	~ 1
	1.9	7.90	2489764 ± 2672	~ 1

CHAPTER 5

CONCLUSION

Unparticle physics is one of the beyond Standard Model scenario introduced by Georgi [3] about a decade ago. It relies on a scale invariance symmetry and it is made possible to interact with the Standard Model through effective operators.

In the first part of the thesis, a detailed discussion of the theory behind the idea of unparticle scenario, including conformal transformations and the group structure as well as very basics of effective field theory. Then the unparticle setting is introduced in details, mainly concentrating on the most unconventional parts like the propagator of scalar unparticle, the phase space including determination of some Feynman rules as well as scalar unparticle three-point self interaction etc. The unparticle effects at colliders are planned to be searched through virtual scalar unparticle contributions.

In the second part of the thesis, various signals like 4 photons, 4 gluons, 4 leptons, 2 gluons + 2 photon2, and 2 photons + 2 leptons at Compact Linear Collider with 3 TeV center of mass energy were examined through scalar unparticle scenario. Possible contributions to these signals may come from three point unparticle self interaction as well as single and double unparticle exchange diagrams.

The signals considered above are analyzed after putting some cuts and results were compared with the background predictions. The number of events with integrated luminosity $\mathcal{L} = 2000\,\mathrm{fb}^{-1}$ and the polarization of electron and positron ($P_{e^-} = 80\%$ and $P_{e^+} = 30\%$) was plotted as a function of kinematic variables like $\Delta R, \eta,$ and p_T. The summary of the results with the significance of each signal was presented in Table 4.3. Cross section was calculated for each signal. The number of signal events (S) have demonstrated and $S/(S+B)$ ratio (B is the number of background events)

was also computed for each signal. As it can be seen from the Table 4.3, $e^-e^+ \to 4\gamma$ seems to be the most promising process as its ratio is around 0.94 which is relatively close to unity. It can be also noted that $e^-e^+ \to 4g$ and $e^-e^+ \to 2g2\gamma$ processes are practically background free at tree level. Even if there can be contributions at one loop level, we should emphasize that it is beyond the scope of this thesis. This analysis and results could be a guidance to identify the existence of unparticle stuff once CLIC data is available.

REFERENCES

[1] S. Chatrchyan *et al.*, "Observation of a New Boson at a Mass of 125 GeV with the CMS Experiment at the LHC," *Phys. Lett.*, vol. B716, pp. 30–61, 2012.

[2] G. Aad *et al.*, "Observation of a new particle in the search for the Standard Model Higgs boson with the ATLAS detector at the LHC," *Phys. Lett.*, vol. B716, pp. 1–29, 2012.

[3] H. Georgi, "Unparticle physics," *Phys. Rev. Lett.*, vol. 98, p. 221601, 2007.

[4] H. Georgi, "Another odd thing about unparticle physics," *Phys. Lett.*, vol. B650, pp. 275–278, 2007.

[5] H. Georgi and Y. Kats, "An Unparticle Example in 2D," *Phys. Rev. Lett.*, vol. 101, p. 131603, 2008.

[6] J. Bergstrom and T. Ohlsson, "Unparticle Self-Interactions at the Large Hadron Collider," *Phys. Rev.*, vol. D80, p. 115014, 2009.

[7] J. L. Feng, A. Rajaraman, and H. Tu, "Unparticle self-interactions and their collider implications," *Phys. Rev.*, vol. D77, p. 075007, 2008.

[8] K. Cheung, W.-Y. Keung, and T.-C. Yuan, "Collider signals of unparticle physics," *Phys. Rev. Lett.*, vol. 99, p. 051803, 2007.

[9] K. Cheung, W.-Y. Keung, and T.-C. Yuan, "Collider Phenomenology of Unparticle Physics," *Phys. Rev.*, vol. D76, p. 055003, 2007.

[10] M. Luo and G. Zhu, "Some phenomenologies of unparticle physics," *Phys. Lett.*, vol. B659, pp. 341–344, 2008.

[11] H. Georgi and Y. Kats, "Unparticle self-interactions," *JHEP*, vol. 02, p. 065, 2010.

[12] M. F. Wondrak, P. Nicolini, and M. Bleicher, "Unparticle contribution to the hydrogen atom ground state energy," *Phys. Lett.*, vol. B759, pp. 589–592, 2016.

[13] A. M. Frassino, P. Nicolini, and O. Panella, "Unparticle Casimir effect," *Phys. Lett.*, vol. B772, pp. 675–680, 2017.

[14] Y. Gong and X. Chen, "Cosmological constraint on unparticle dark matter," *Eur. Phys. J.*, vol. C57, pp. 785–789, 2008.

[15] T. Kikuchi and N. Okada, "Unparticle Dark Matter," *Phys. Lett.*, vol. B665, pp. 186–189, 2008.

[16] M. A. Stephanov, "Deconstruction of Unparticles," *Phys. Rev.*, vol. D76, p. 035008, 2007.

[17] G. Cacciapaglia, G. Marandella, and J. Terning, "The AdS/CFT/Unparticle Correspondence," *JHEP*, vol. 02, p. 049, 2009.

[18] H. Davoudiasl, "Constraining Unparticle Physics with Cosmology and Astrophysics," *Phys. Rev. Lett.*, vol. 99, p. 141301, 2007.

[19] I. Lewis, "Cosmological and Astrophysical Constraints on Tensor Unparticles," 2007.

[20] J. McDonald, "Cosmological Constraints on Unparticles," *JCAP*, vol. 0903, p. 019, 2009.

[21] A. Karch, K. Limtragool, and P. W. Phillips, "Unparticles and Anomalous Dimensions in the Cuprates," *JHEP*, vol. 03, p. 175, 2016.

[22] Z. Leong, C. Setty, K. Limtragool, and P. W. Phillips, "Power-law liquid in cuprate superconductors from fermionic unparticles," *Phys. Rev.*, vol. B96, no. 20, p. 205101, 2017.

[23] K. Limtragool, C. Setty, Z. Leong, and P. W. Phillips, "Realizing infrared power-law liquids in the cuprates from unparticle interactions," *Phys. Rev.*, vol. B94, no. 23, p. 235121, 2016.

[24] A. M. Sirunyan *et al.*, "Search for dark matter and unparticles in events with a Z boson and missing transverse momentum in proton-proton collisions at $\sqrt{s} = 13$ TeV," *JHEP*, vol. 03, p. 061, 2017. [Erratum: JHEP09,106(2017)].

[25] V. Khachatryan *et al.*, "Search for dark matter and unparticles produced in association with a Z boson in proton-proton collisions at $\sqrt{s} = 8$ TeV," *Phys. Rev.*, vol. D93, no. 5, p. 052011, 2016. [Erratum: Phys. Rev.D97,no.9,099903(2018)].

[26] P. Di Francesco, P. Mathieu, and D. Sénéchal, *Conformal field theory*. Graduate texts in contemporary physics, New York, NY: Springer, 1997.

[27] G. Mack, "All unitary ray representations of the conformal group SU(2,2) with positive energy," *Commun. Math. Phys.*, vol. 55, p. 1, 1977.

[28] A. V. Manohar, "Introduction to Effective Field Theories," in *Les Houches summer school: EFT in Particle Physics and Cosmology Les Houches, Chamonix Valley, France, July 3-28, 2017*, 2018.

[29] A. Pich, "Effective field theory: Course," in *Probing the standard model of particle interactions. Proceedings, Summer School in Theoretical Physics, NATO Advanced Study Institute, 68th session, Les Houches, France, July 28-September 5, 1997. Pt. 1, 2*, pp. 949–1049, 1998.

[30] S. Rychkov, *EPFL Lectures on Conformal Field Theory in D>= 3 Dimensions*. SpringerBriefs in Physics, 2016.

[31] T. Banks and A. Zaks, "On the Phase Structure of Vector-Like Gauge Theories with Massless Fermions," *Nucl. Phys.*, vol. B196, pp. 189–204, 1982.

[32] L. S. Brown, *Structural aspects*, p. 282–353. Cambridge University Press, 1992.

[33] S.-L. Chen and X.-G. He, "Interactions of Unparticles with Standard Model Particles," *Phys. Rev.*, vol. D76, p. 091702, 2007.

[34] T. Han, "Collider phenomenology: Basic knowledge and techniques," in *Physics in D >= 4. Proceedings, Theoretical Advanced Study Institute in elementary particle physics, TASI 2004, Boulder, USA, June 6-July 2, 2004*, pp. 407–454, 2005.